

Progress and Perspective on Rechargeable Magnesium–Sulfur Batteries

Yan Lu, Cong Wang, Qiang Liu, Xiaoyan Li, Xinyu Zhao,* and Zaiping Guo*


Rechargeable magnesium–sulfur (Mg–S) batteries are emerging as a promising candidate for next-generation energy storage technologies owing to their prominent advantages in terms of high volumetric energy density, low cost, and enhanced safety. However, their practical implementation is facing great challenges in finding electrolytes that can fulfill a multitude of rigorous requirements along with efficient sulfur cathodes and magnesium anodes. This review highlights electrolyte design for reliable Mg–S batteries in terms of efficient Mg-based salt construction (cation/anion design of organomagnesium salt-based electrolytes, optimization of all inorganic salt-based electrolytes and choosing of simple salt-based electrolytes), suitable solvent selection, and strategies for confronting corrosivity of Mg electrolytes. Before the comprehensive overview of the research status of Mg-based electrolytes, the understanding of Mg–S electrochemistry and views on the recent progress and potential strategies for high-performance S-based cathode and Mg anode are also provided for a holistic insight into Mg–S systems. At the end, the perspectives on the possible research directions for constructing high performance practical Mg–S batteries are also shared.

Dr. Y. Lu, C. Wang, Q. Liu
Center of Nanoelectronics
School of Microelectronics
Shandong University
Jinan 250100, P. R. China

Dr. X. Li
Laboratoire de Physique des Solides
Bâtiment 510
Université Paris-Saclay
Orsay 91405, France

Dr. X. Zhao
School of Materials Science and Engineering
Shandong University of Technology
Zibo 255000, P. R. China
E-mail: zhaoxinyu@sdut.edu.cn

Prof. Z. Guo
School of Mechanical
Materials
Mechatronic and Biomedical Engineering
Australian Institute for Innovative Materials
Institute for Superconducting & Electronic Materials
University of Wollongong
Wollongong, NSW 2522, Australia
E-mail: zguo@uow.edu.au

 The ORCID identification number(s) for the author(s) of this article can be found under <https://doi.org/10.1002/smt.202001303>.

DOI: 10.1002/smt.202001303

1. Introduction

The ever-growing energy demand and challenging environmental issues impose a great pressure on the society to develop sustainable energy alternatives to the depleting fossil-fuel resources.^[1] Over the past three decades, rechargeable lithium-ion batteries (LIBs) have achieved great success in the portable electronics market and have become one of the most successful sustainable energy technologies.^[1c,2] However, the development of large-scale applications (electric vehicles, stationary applications) requires better performance from energy-storage devices. Furthermore, LIBs are reaching their ceiling capacity due to the limitations of the conventional “rocking-chair” mechanism, thus limiting them from meeting ever-increasing energy demands.^[3] It is therefore essential to explore novel battery chemistries to power our future society.

Lithium–sulfur (Li–S) batteries, using sulfur to replace intercalation-type cathode, have been regarded as

an intriguing alternative to state-of-the-art LIBs.^[4] Based on the two-electron redox reaction of sulfur, the Li–S technology could deliver a high energy density of 2600 Wh kg^{−1} or 2800 Wh L^{−1}, which is much higher than that of LIBs.^[5] Being extensively studied since 2009,^[6] Li–S batteries have achieved remarkable progress and demonstrated practical performance in some niche applications, such as electric bicycles, and test applications.^[5c] Nevertheless, the long-term sustainability of Li–S technology is a great concern due to the limited reserves and geographic scarcity of lithium resource in the earth's crust. As a result, nonlithium-metal based sulfur batteries utilizing more abundant elements (e.g., sodium, potassium, magnesium, aluminum, zinc) have attracted considerable attentions, especially for large-scale applications, where price per kWh precedes power considerations.^[7] Notably, despite extensive progress in sodium (Na)-based and potassium (K)-based sulfur batteries, key challenges are faced such as the inevitable formation of metallic dendrites during cycling processes, which can induce internal short-circuits and cause severe safety problems.^[5c,8] On the contrary, magnesium (Mg) anodes possess better safety properties because they do not easily form dendrites, making them competitive candidates to construct the next-generation high-performance metal–sulfur batteries.

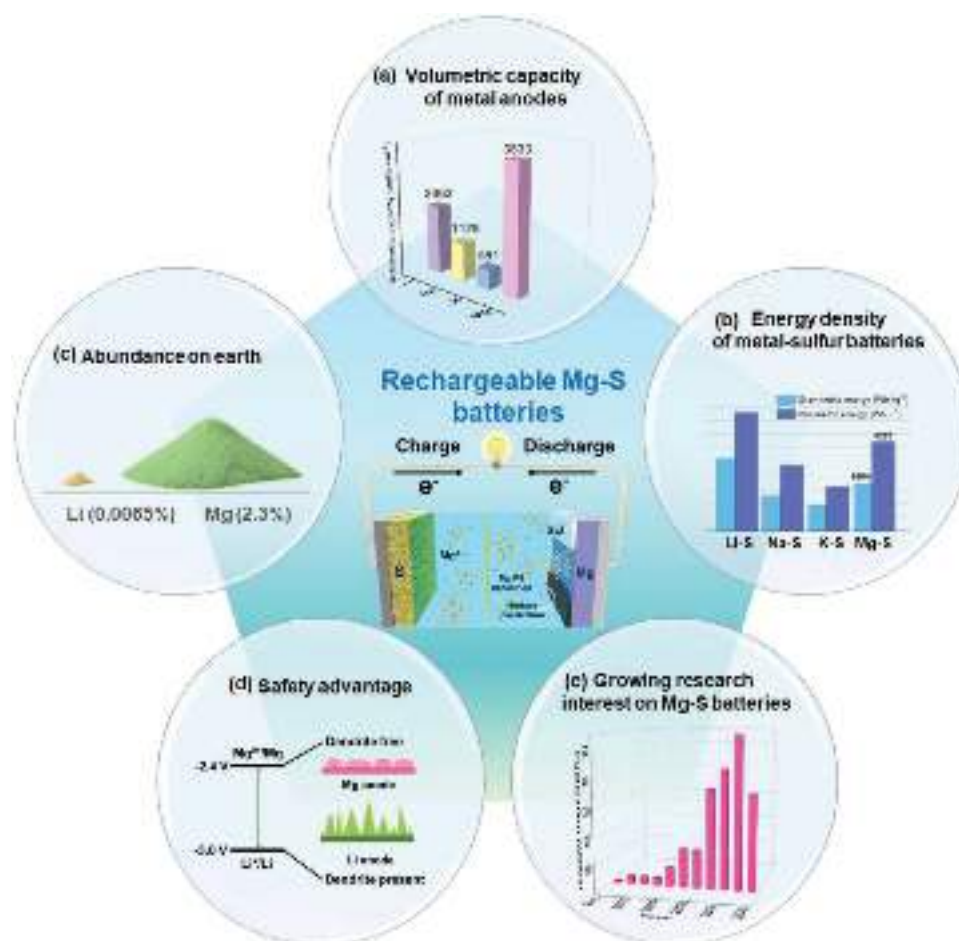


Figure 1. Comparison of a) volumetric capacity for Li, Na, K, Mg metal anodes, b) energy density of Li-S, Na-S, K-S, Mg-S batteries and c) abundance of Li and Mg in the Earth's crust; d) safety advantage of Mg anodes versus Li anodes; e) number of published articles on Mg-S batteries since 2010.

In addition to its safety superiority, Mg also has other merits, which triggers the research interest in Mg-based rechargeable batteries.^[9] To be specific, Mg has a much higher volumetric capacity of 3833 mAh cm⁻³ than those of alkaline metal anodes (2062 mAh cm⁻³ for lithium, 1128 mAh cm⁻³ for sodium, and 591 mAh cm⁻³ for potassium), rendering it an excellent choice for high-energy density batteries with reduced pack size^[10] (Figure 1a). Furthermore, Mg can be safely operated in air and has a relative low reduction potential of -2.4 V versus standard hydrogen electrode.^[11] Most importantly, the successful coupling of Mg anode with S cathode endows Mg-S system with distinct advantages, such as relatively high energy densities (1684 Wh kg⁻¹ or 3221 Wh L⁻¹),^[11a] resulting from the combination of the divalent feature of Mg ions and conversion mechanism of sulfur (Figure 1b). Other advantages of Mg and S are their low-cost and high sustainability for large-scale applications because of their abundance in the earth's crust and ready availability in various minerals (Figure 1c).^[9a,10] Furthermore, cells based on these two elements are expected to demonstrate high safety and long cycle-life benefitting from the absence of metal dendrites (Figure 1d) and a smaller volume expansion for the formed sulfides (24% for MgS vs 72% for Li₂S).^[10] Given the great promise of the Mg-S system as a potential future battery

technology with low-cost, high energy density and enhanced safety, a noticeable increase in publications featuring Mg-S batteries has been witnessed in recent years (see Figure 1e).

Nevertheless, compared with the remarkable progress of Li-S batteries, the R&D on Mg-S batteries is still in an early stage. The key technical obstacle impeding its development is the lack of suitable electrolytes, which are required to be chemically compatible to the electrophilic S and capable of realizing reversible Mg deposition/dissolution.^[10,12] This is quite challenging as most of the commercially available Mg analogues of Li salts in aprotic solvents can hardly meet these requirements, and thus extensive efforts are required for the delicate design and innovative synthesis of applicable Mg salts and solvents specifically suited to Mg-S batteries. Further, the attaining of high-performance S-based cathodes is a prerequisite to realize practical Mg-S batteries. However, a series of issues, such as low-intrinsic conductivity of sulfur, the dissolution of intermediary polysulfides, the formation of electrochemically inactive final products (MgS and MgS₂),^[9a,13] need to be addressed to achieve practical S-based cathodes. Moreover, the slow diffusion of Mg²⁺ demands special attention for transport pathway design in electrolyte and electrodes. Additionally, electrode/electrolyte interface optimization is required to guarantee the

reaction kinetics and promote the successful operation and high energy output of Mg–S batteries. In addition, fundamental understanding of electrode/electrolyte interfacial electrochemistry and individual redox reactions during charge–discharge are crucial to further improve cell performance.

The purpose of this review is to provide a comprehensive overview of the research status of Mg–S batteries, summarizing recent progress and highlighting novel findings. To begin, the working principle and electrochemistry behind the battery reactions of the Mg–S system is introduced and the challenges it is facing are elaborated. Then, materials involved in sulfur-based cathodes are presented and strategies for the performance improvement of cathodes are highlighted. Further, various forms of Mg anodes are examined, and prospective anodes are proposed. After that, electrolyte systems are thoroughly explained in detail in this review. The electrolyte-related section includes a detailed discussion of the basic understanding of Mg electrolytes and a systematic summary of the design strategies for Mg electrolytes in terms of Mg salts construction (cation/anion design in organomagnesium salt-based electrolytes, all inorganic salts choosing and simple salts adopting) and solvents selection. In addition, corrosion issue of other metallic components in batteries by the designed Mg electrolytes is also discussed and in our conclusions, we share our view on the existing challenges and future research directions for high-performance Mg–S batteries.

2. Mg–S Electrochemistry

A Mg–S battery is composed of a Mg metal anode, a sulfur-based cathode, an organic electrolyte, and a separator. During the discharging process, Mg metal is oxidized to Mg^{2+} ions accompanied by reduction of sulfur by electrons that are transported from the Mg anode to the sulfur cathode through an external electrical circuit. The successive reduction of sulfur forms Mg polysulfides with various chain lengths. The formation process of Mg polysulfides is similar to that of Li polysulfides in Li–S batteries. The different properties of Mg polysulfides, however, such as solubility, electrochemical activity, and Mg^{2+} ion transport rate in Mg polysulfides, make the electrochemistry of Mg–S batteries different from that of Li–S batteries. Understanding the electrochemistry including thermodynamics and kinetics is crucial for developing Mg–S batteries with enhanced performance. To this end, several research groups have conducted mechanistic studies of sulfur reaction with Mg through combined experimental and computational methods.^[13,14] In this section, their research results on the reaction processes and mechanisms are reviewed.

Gao et al. used three-electrode cells with Mg metal as both counter and reference electrodes and sulfur as cathode to eliminate the polarization of Mg.^[13] Unlike the large voltage hysteresis reported in some two-electrode cells, the voltage hysteresis between the discharge/charge curve in their three-electrode system was very small (<0.2 V for the plateau). As the three-electrode system only reflects the sulfur overpotential, therefore the authors inferred that the large voltage hysteresis in two-electrode cells is presumably due to the anode overpotential. This inference is consistent with the conclusion of another

study on Mg–S battery impedance.^[14a] Vinayan et al. found that anode impedance (from 759 to 1292 $\Omega \text{ cm}^{-2}$) increased much faster than the cathode impedance (from 190 to 265 $\Omega \text{ cm}^{-2}$) under open circuit potential, indicating that the total Mg–S battery impedance is dominated by the anode impedance.

By examining the forms of polysulfides existing in the Mg–S electrolyte during discharge using characterization methods including electrospray-ionization mass spectrometry and in situ Raman spectra (Figure 2a,b), the whole sulfur reduction process can be divided into three stages (Figure 2c,d).^[13,14] In stage I, the elemental sulfur is partially reduced to MgS_8 through a solid–liquid two-phase reaction, corresponding to the sloping potential of 2.5–1.5 V in the discharge curve



In stage II, MgS_8 is successively reduced to short chain MgS_2 through gradual chain-shortening of the polysulfides, corresponding to the potential plateau at 1.5 V. As the solubility of MgS_x ($x = 8-4$) is small ($<50 \times 10^{-3}$ M, so MgS_2 could be termed “insoluble”), most sulfur species should exist in the solid phase with a Mg concentration gradient within it. Nevertheless, a small portion of long chain polysulfides that dissolve in the electrolyte easily diffuses to sites where electrons are more available and can be further reduced. Then, the further reduced polysulfides migrate to other surface sites to reduce to undissolved MgS_x through a disproportion reaction. This surface magnesiation constitutes one pathway for sulfur reduction^[13]



In stage III, the depletion of soluble long-chain polysulfide MgS_x ($x = 8-4$) causes the bulk magnesiation, another sulfur reduction pathway, to start via the diffusion of Mg^{2+} ions from the electrolyte to the solid-state MgS_x and S. The Mg^{2+} ion diffusivity within Mg polysulfides decreases with the decrease in the chain length. As MgS_x ($x = 2-8$) tends to exist in an amorphous phase, the ion diffusivity is much higher in MgS_x ($x = 2-8$) than that in crystalline MgS (Figure 2e). Therefore, once MgS forms at the interface, the low ion diffusivity causes large overpotential with slow kinetics, leading to a sharp potential drop from 1.5 to 0.5 V and early termination of discharge^[13]



Notably, complete recharge is not possible even under the same equilibrium condition and a capacity loss is observed (Figure 2d). This is ascribed to the poor reversibility of formed (poly)sulfide and the loss of active material due to the dissolution of S and MgS_x .^[13]

The effects of sulfur to carbon ratio (S/C) in cathodes during the discharge process were also analyzed using the above sulfur reduction pathways.^[13] At high S/C ratios (i.e., high sulfur loading), only a thin surface layer of sulfur can be dissolved into the electrolyte, due to the low solubility of Mg polysulfides, thereby forcing most sulfur species to remain in the solid state. When the dissolved polysulfide mediators are all depleted, the reduction reaction enters stage III and the potential drops quickly to an end, leaving most bulk sulfur not fully reduced.

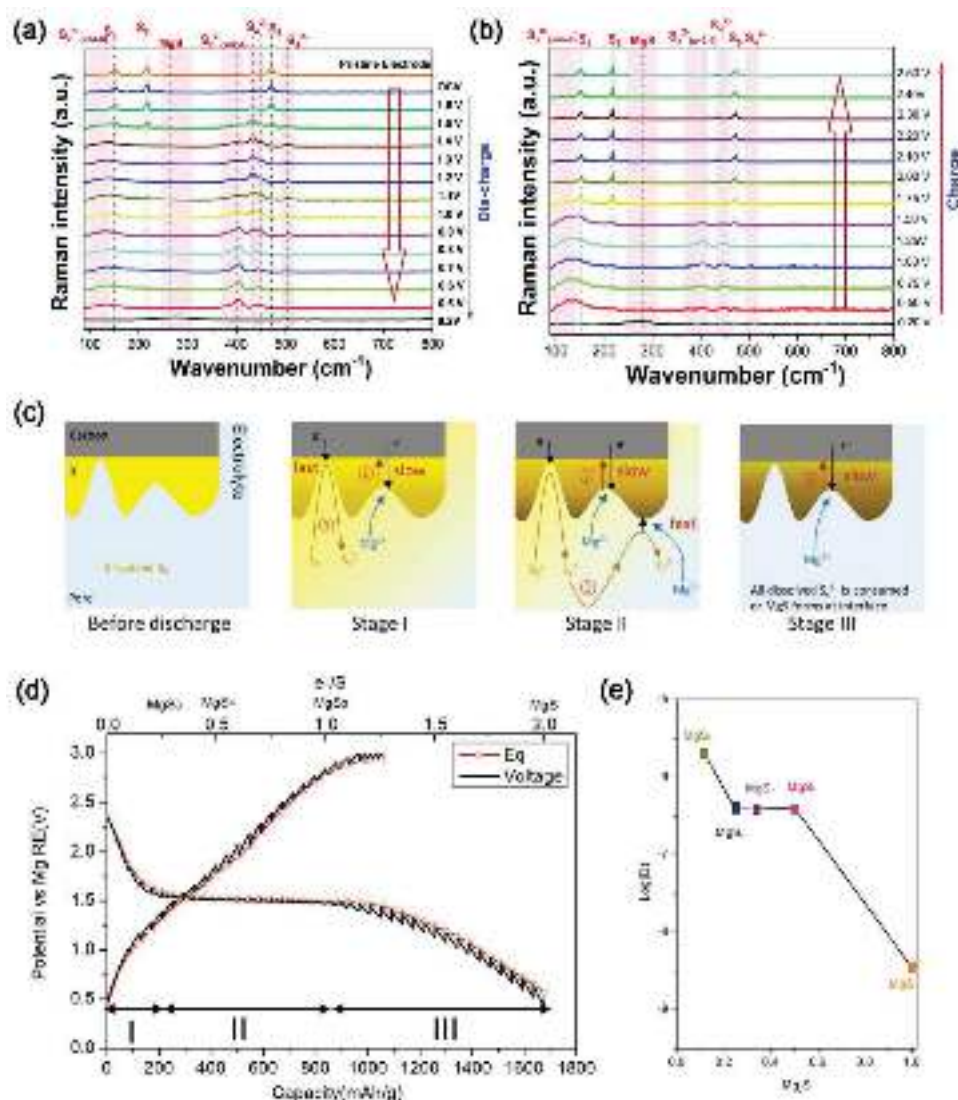


Figure 2. In Operando Raman spectra of the S/N-doped carbon cathode in a Mg–S battery during a) discharge and b) charge processes. Reproduced with permission.^[14a] Copyright 2019, The Royal Society of Chemistry. c) Sulfur reduction mechanism for three stages. d) Thermodynamic equilibrium potential with different Mg polysulfides marked in three stages. Red: equilibrium curve; Black: transient potential. e) Calculated diffusivities of Mg^{2+} in Mg polysulfides and MgS at 600 K. Reproduced with permission.^[13] Copyright 2018, Wiley-VCH.

Therefore, low capacity (i.e., low utilization of sulfur) is usually observed under a high S/C ratio. In contrast, highly soluble Li polysulfides endow continuous dissolution of surface sulfur to expose and reduce more bulk sulfur, enabling high utilization of sulfur under a high S/C ratio.

In addition to the investigations of the detailed reaction pathways for Mg–S batteries, researchers also studied the origin of fast capacity loss in Mg–S batteries. For example, Xu et al. revealed a possible reason for the capacity fading by analyzing the chemical species in the cathode using an in situ X-ray absorption spectroscopic (XAS).^[14b] They first divided the sulfur reduction into three stages: 1) fast formation of long chain Mg polysulfides (e.g., MgS_8 , MgS_4); 2) formation of a stable Mg_3S_8 phase by reduction of long chain Mg polysulfides; and 3) further reduction of Mg_3S_8 to MgS. Then, they ascribed the capacity fading to the formation of electrochemically inert

Mg_3S_8 and MgS, which are difficult to revert back to long chain Mg polysulfides. After their results analysis, they proposed introducing TiS_2 as a catalyst to activate the short chain Mg polysulfides by coating it on the separator. By doing so, Mg–S battery can achieve an improved capacity (i.e., 900 mAh g^{-1}) and a better cyclability.

Despite the extensive research efforts studying the mechanisms of Mg–S system, its practical implementation still faces some critical technical challenges associated with both materials and system, which mainly involve the following aspects: 1) the insulating nature of sulfur and Mg-based polysulfide/sulfide, which results in low utilization of the active material and electrode passivation, harmful for the achieving a practical capacity; 2) the lack of suitable electrolytes, which are required to be compatible with both sulfur cathodes and Mg anodes, and meanwhile can support the transport of divalent Mg^{2+}

ions; 3) sluggish reduction kinetics of MgS_2 to MgS , which leads to a large overpotential and severe reversible capacity loss at low cut-off voltage; 4) the formation of passivation layer/solid electrolyte interphase (SEI) on Mg anode due to the possible reaction between Mg anode and electrolyte and the deposition of insoluble Mg polysulfides/sulfides, which is harmful for achieving long-term cycling stability in the Mg–S system.

To address the challenges mentioned above, extensive efforts have been devoted to promoting the reaction kinetics of S-based cathodes, constructing desirable electrolyte systems, enhancing the reversible transformation of MgS_2 to MgS , and avoiding the passivation/SEI layer formation on Mg anodes. Approaches focusing on cathode architecture design, Mg anode protection, and suitable-electrolyte construction have been explored, and notable progress has been achieved. Representative examples of these approaches will be discussed in Sections 3–5.

3. Cathodes

Sulfur as the active material in Mg–S cathodes has many advantages including low cost, nontoxicity, and high theoretical energy density (1675 mAh g^{-1}).^[15] With a suitable conversion mechanism, sulfur is an ideal cathode matching with Mg anodes, which circumvents the shortcomings of divalent Mg^{2+} with intrinsically slow kinetics in intercalation cathodes. As in other metal-sulfur batteries, such as Na–S and K–S, cathode knowledge developed in Li–S system can be cautiously imported into Mg–S system. For example, porous, conductive carbonaceous materials are employed as supports for sulfur in various metal-sulfur batteries to improve the utilization of insulating sulfur, accommodating volume expansion and reducing the dissolution of polysulfides.^[5c] In addition, battery configuration design that aims to control the polysulfides dissolution and diffusion from cathode to electrolyte can generally help improve cathode performance.

3.1. Carbonaceous Materials for Mg–S Cathodes

Conductive matrix is an essential component in sulfur cathodes. Without a conductive matrix, pure sulfur cathodes suffer rapid capacity fading from the first discharge (e.g., 111 mA h g^{-1}) to the 3rd discharge (2 mA h g^{-1}) and battery fails after further cycles.^[16] To achieve an improved performance, carbonaceous matrices are required to intimately contact with the active sulfur material and intermediate products. Moreover, high mechanical stability is necessary to accommodate the large volume changes during the conversion reactions. For this reason, conductive matrices with good electrical conductivity, high porosity, and flexibility are good choices. Generally, such carbonaceous materials include activated carbon cloth (ACC), graphene-based matrices, carbon nanotubes (CNTs), carbon nanofibers (CNFs), sulfur graphdiyne (SGDY), and nanoporous carbon (e.g., CMK-3) (see summary in Table 1).^[14a,17] Given the existing forms of sulfur in the cathode (S_8 ; small sulfur molecule S_n , $n \leq 4$; and metal-based polysulfides), different sulfur loading methodologies have been well established for carbonaceous matrices. Specifically, S_8 is usually obtained by impregnating sulfur into

microporous or mesoporous carbon substrates at a temperature above the melting point of sulfur (e.g., 155°C).^[5c] Small sulfur molecules have been prepared by virtue of the confinement of micropores within microporous carbonaceous matrices. Differing from S_8 and small sulfur molecules, Mg-based polysulfides are synthesized via reactions between sulfur and Mg metal in organic solvent.^[17b] In contrast to S_8 , small sulfur molecules and metal-based polysulfides display higher reactivity and more homogeneous distribution on carbon matrices. In this section, typical examples of S-based cathodes for Mg–S system will be discussed and the challenges facing Mg–S cathode, as well as the some demonstrated solutions will also be given.

3.1.1. ACC

In the first report of a Mg–S battery, Kim et al. prepared the cathode by simply coating a mixture of elemental sulfur, carbon black and poly(tetrafluoroethylene) binder on a porous carbon substrate.^[17a] Their sulfur loading is 61 wt%. Through analyzing their sulfur cathodes using X-ray photoelectron spectroscopy (XPS) after charging and discharging, they found that the cathode was plagued with similar challenges as experienced in Li–S batteries, which was dissolution of sulfur and polysulfide into the electrolyte.

3.1.2. Graphene and CNTs

Vinayan et al. prepared a nitrogen-doped hybrid nanocomposite of multiwall carbon nanotubes (MWCNTs) and graphene as a substrate loaded with different amounts of sulfur (with $0.5\text{--}3 \text{ mg cm}^{-2}$) as cathodes.^[14a] The MWCNTs have multiple functions in the cathode substrate, including: 1) preventing graphene sheets from restacking, thereby maintaining a large specific surface area (i.e., $644 \text{ m}^2 \text{ g}^{-1}$) and 2) improving electronic conductivity. In addition, the authors used nitrogen plasma to introduce N dopant into the substrate, which increases the binding strength of polysulfides to the N-doped substrate through S–N bonding. The designed cathode with high surface area had a high sulfur loading of $\approx 76.2 \text{ wt\%}$, however, it showed rapid capacity fading when compared to samples with a lower sulfur loading of 20 wt%. This unusual phenomenon was ascribed to the augmented loss of sulfur active material and polysulfides during cycling.^[14a]

Xu et al. employed Mg polysulfide as active materials (i.e., catholyte) and graphene/carbon nanotube (G-CNT) as carbon matrix to prepare cathodes (see Figure 3).^[17b] Their homogeneously distributed polysulfide cathode with high reactivity achieved a high discharge capacity ($>1000 \text{ mAh g}^{-1}$) and a long cycle-life (>50 cycles) when coupled with a newly designed $\text{MgCl}_2\text{--YCl}_3$ electrolyte.^[17b] The Mg polysulfide was synthesized by the reaction of Mg and S powders in a ratio of 1:8 in a basic solvent of N-methylimidazole (N-MeIm) at 95°C .^[18] Cathodes were obtained by dropping the MgS_8 solution onto G-CNT pasted pyrolytic graphite substrate. These polysulfide cathodes required an activation process leading to slightly lower capacities in the first few cycles. Their discharge/charge plateaus were at 1.2 and 2.2 V.^[17b]

Table 1. Summary of properties of currently reported Mg–S batteries based on different S/C cathodes.

Carbon materials in cathode	Cathode	Sulfur loading	Electrolyte	Initial discharge capacity [mAh g ⁻¹]	Remaining discharge capacity [mAh g ⁻¹]	Cycle number	Ref.
Activated carbon cloth (ACC)	S@carbon Black and PTFE binder on porous carbon substrate	61 wt%	[Mg ₂ (μ-Cl) ₃ 6THF] [HMDSAICl ₃]/THF	1200	394	2	[17a]
	S@ACC	15 wt% (0.5 mg cm ⁻²)	0.1 M (HMDS) ₂ Mg–2AlCl ₃ + 1 M LiTFSI	≈500	1000	30	[45]
	S@ACC	1 mg cm ⁻²	1 M Mg(TFSI) ₂ –MgCl ₂ in DME	≈800	≈700	110	[24b]
	S@ACC with CNF-coated separator	1 mg cm ⁻²	Mg[B(hfp) ₄] ₂ in DME	930	≈200	100	[58]
Graphene and carbon nanotube (CNT)	S@N-doped-graphene	50 wt%	[Mg(THF) ₆][AlCl ₄] ₂ / PYR14TFSI in THF	700	40	20	[60]
	S@rGO	49 wt%	(HMDS) ₂ Mg–2AlCl ₃ – MgCl ₂ in tetraglyme	1024	219	50	[16]
	S@CNT	1 mg cm ⁻²	0.5 M [Mg ₄ Cl ₆ (DME) ₆][B(HFP) ₄] ₂	1247	1019	100	[54]
	S@rGO with N,S doped carbon cloth current collector and CNF coated separator	1 mg cm ⁻²	(HMDS) ₂ Mg–2AlCl ₃ – MgCl ₂ in tetraglyme	≈1000	388	40	[78]
	MgS ₈ @Graphene-CNT	0.7–1 mg cm ⁻²	MgCl ₂ –YCl ₃ in PYR ₁₄ TFSI and DG	≈1200	≈1000	50	[17b]
	S@Graphene-CNT	3 mg cm ⁻² ; 0.5 mg cm ⁻²	0.4 M Mg[B(hfp) ₄] ₂ in DME solvent	431 for 3 mg cm ⁻² ; 1384 for 0.5 mg cm ⁻² ;	228 for 3 mg cm ⁻² at cycle 50; 1117 for 0.5 mg cm ⁻² at cycle 5;	50	[14a]
Microporous carbon	S@mesoporous carbon	85 wt%	0.5 M THFPB + 0.05 M MgF ₂ in DME	1081	≈900	30	[53]
	S@CMK-3	69.3 wt%	0.3 M Mg(TFSI) ₂ /in DME and diglyme	500	100	4	[61]
	S@CMK-3	55 wt%	1.2 M (HMDS) ₂ Mg–2AlCl ₃ –MgCl ₂ in diglyme or tetraglyme/PP14TFSI	800	260	20	[24c]
	S@CMK-3	1 mg cm ⁻²	0.8 M Mg[B(hfp) ₄] ₂ in diglyme and tetraglyme	800	200	100	[51]
	S@microporous carbon	64.7 wt%	0.4 M (PhMgCl) ₂ –AlCl ₃ and 1 M LiCl in THF	979	368.8	200	[19]
	S@microporous carbon	55 wt%	Mg(CF ₃ SO ₃) ₂ –AlCl ₃ in tetraglyme and THF	1200	400	50	[67a]
	S@microporous carbon	55.8 wt%	Mg bis(diisopropyl) amide MBA–AlCl ₃ –LiCl in THF	700	400	100	[47]
	S@MOF derivative carbon	1 mg cm ⁻²	(HMDS) ₂ Mg–2AlCl ₃ with LiTFSI	600	400	200	[21]
Sulfide graphdiyne (SGDY)	S@SGDY	1 mg cm ⁻²	(PhMgCl) ₂ –AlCl ₃ and LiCl in THF	1124	459	36	[17c]
Carbon nanofiber (CNF)	S@CNF with CNF coated separator	50 wt%	HMDSMgCl	1200	800	20	[24a]
Sulfur containing composite	S@BUMB18C6 And S@UOEE	No data	0.5 M Mg(TFSA) ₂ in triglyme or acetonitrile	460 for S@BUMB18C6; 495 for S@UOEE	68.1 for S@BUMB18C6; 0.18 for S@UOEE	10	[79]
	S with functional separator (CuNWs-GN/PI/LLZO membrane)	3 mg cm ⁻²	[Mg ₄ Cl ₆ (DME) ₆][B(HFP) ₄] ₂	390	915	25	[62]

3.1.3. Nanoporous Carbon

In 2018, Wang et al. reported a sulfur@microporous carbon (S@MC) cathode for Mg–S batteries.^[19] In the micropores of the host, sulfur that exists in the form of small chain sulfur (i.e., S₂ to S₄) is confined and physically adsorbed. The small

chain sulfur in the micropores undergoes a “solid–solid” reaction mechanism, avoiding the transition from S₈ to S₄²⁻, hence improving the reaction kinetics. Meanwhile, the micropores physically adsorb polysulfides formed upon cycling, alleviating the dissolution and shuttling problems of polysulfides. On the outside surface of the host, sulfur exists in the form

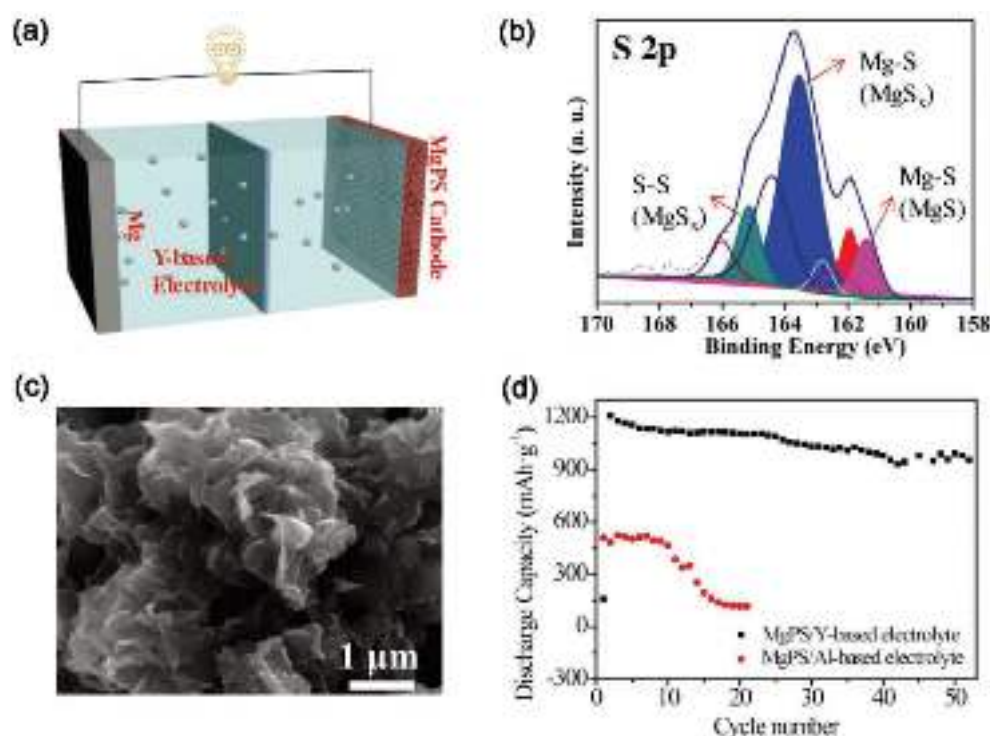


Figure 3. A MgS_8 @graphene-carbon nanotube (MgPS@G-CNT) cathode for a Mg-S battery. a) Schematic illustration of Mg-S battery. b) XPS spectrum of MgPS@G-CNT . c) SEM image of MgPS@G-CNT . d) Cycling stability of the MgPS@G-CNT cathode in different electrolytes. Reproduced with permission.^[17b] Copyright 2019, Wiley-VCH.

of large ring-like S_8 molecules which are reduced to the end member of S^{2-} through a “solid–liquid–solid” reaction mechanism. These S_8 molecules and their polysulfide intermediates were restrained through chemical bonding with a Cu current collector. This strong chemical bonding formed between sulfur and Cu current collector makes the cathode compatible with nucleophilic electrolytes.^[19] Due to the above merits of the designed S@MC cathode, the Mg-S battery showed superior electrochemical performances including high capacity (i.e., $\approx 979 \text{ mAh g}^{-1}$), high capacity retention (i.e., 369 mAh g^{-1} after 200 cycles), high Coulombic efficiency (CE) (i.e., 100%), small overpotential ($< 0.4 \text{ V}$) and an obvious voltage plateau (at $\approx 1.1 \text{ V}$).^[19,20] In 2018, Zhou et al. used a metal organic framework (MOF)-derived carbon matrix prepared sulfur cathode.^[21] A carbon scaffold derived from ZIF-67 was doped by N and Co atoms which can anchor polysulfides via strong bonding with sulfur species. Couple with a $(\text{HMDS})_2\text{Mg}-2\text{AlCl}_3$ electrolyte with LiTFSI additive, the Mg-S battery showed high initial capacity (i.e., 400 mAh g^{-1}), good capacity retention and cyclability (i.e., 400 mAh g^{-1} after 200 cycles), and excellent rate capability ($300\text{--}400 \text{ mAh g}^{-1}$ achievable at a 5 C rate). Their superior performance is attributed to both the rational cathode design (e.g., trapping sites for polysulfides) and the selected electrolyte additive (for removing anode passivation layers).

Very recently in 2020, Sun et al. reported a carbon-confined sulfurized cobalt in a mesoporous matrix (MesoCo@C-S) as a Mg-S cathode (Figure 4).^[22] After in situ sulfurization, a layer of sulfurized CoS_x species was formed on the surface of Co nanoparticles, which provides strong binding to polysulfides.

Both the carbon matrix and the preserved Co cores have excellent electronic conductivity, which promotes charge transfer to the sulfurized CoS_x species and thereby improves the cathode kinetics. Their MesoCo@C-S cathodes had a high initial capacity 830 mAh g^{-1} and retained a capacity of 280 mAh g^{-1} after 400 cycles.

As a typical example of mesoporous carbon substrate for sulfur in Li-S batteries, CMK-3 has also been investigated in Mg-S batteries. Zhao-Karger et al. fabricated a S/CMK400PEG cathode using CMK-3 as the substrate with a 3:7 weight ratio of CMK-3 to sulfur. Benefitting from the large pore volume and interconnected pore structure, CMK-3 could provide a conductive framework for sulfur and constrained space for the electrochemical reaction. When tested in Mg-S battery with a tetraglyme/PP14TFSI electrolyte, S/CMK400PEG cathode delivered a capacity of 800 mA h g^{-1} in the first cycle and a reversible capacity of about 260 mAh g^{-1} after more than 20 cycles.^[24c] Further, Zhao-Karger et al. investigated the compatibility of S/CMK-3 based cathode in the explored $\text{MgBOR(hfip)/diglyme-tetraglyme}$ (DEG-TEG) electrolyte and a reversible discharge capacity of about 200 mAh g^{-1} was retained after 100 cycles, indicating a good cycling stability.^[51] Ha et al. reported a Mg/CMK3-S cell with 0.3 M Mg(TFSI)_2 in glyme/diglyme, which exhibited a discharge capacity of 500 mAh g^{-1} and a potential plateau of 0.2 V . However, this cell still suffers from the shuttle phenomenon due to the high solubility of polysulfides, which required further modification of a CMK-3 mesoporous carbon/sulfur composite cathode to mitigate the shuttle mechanism.

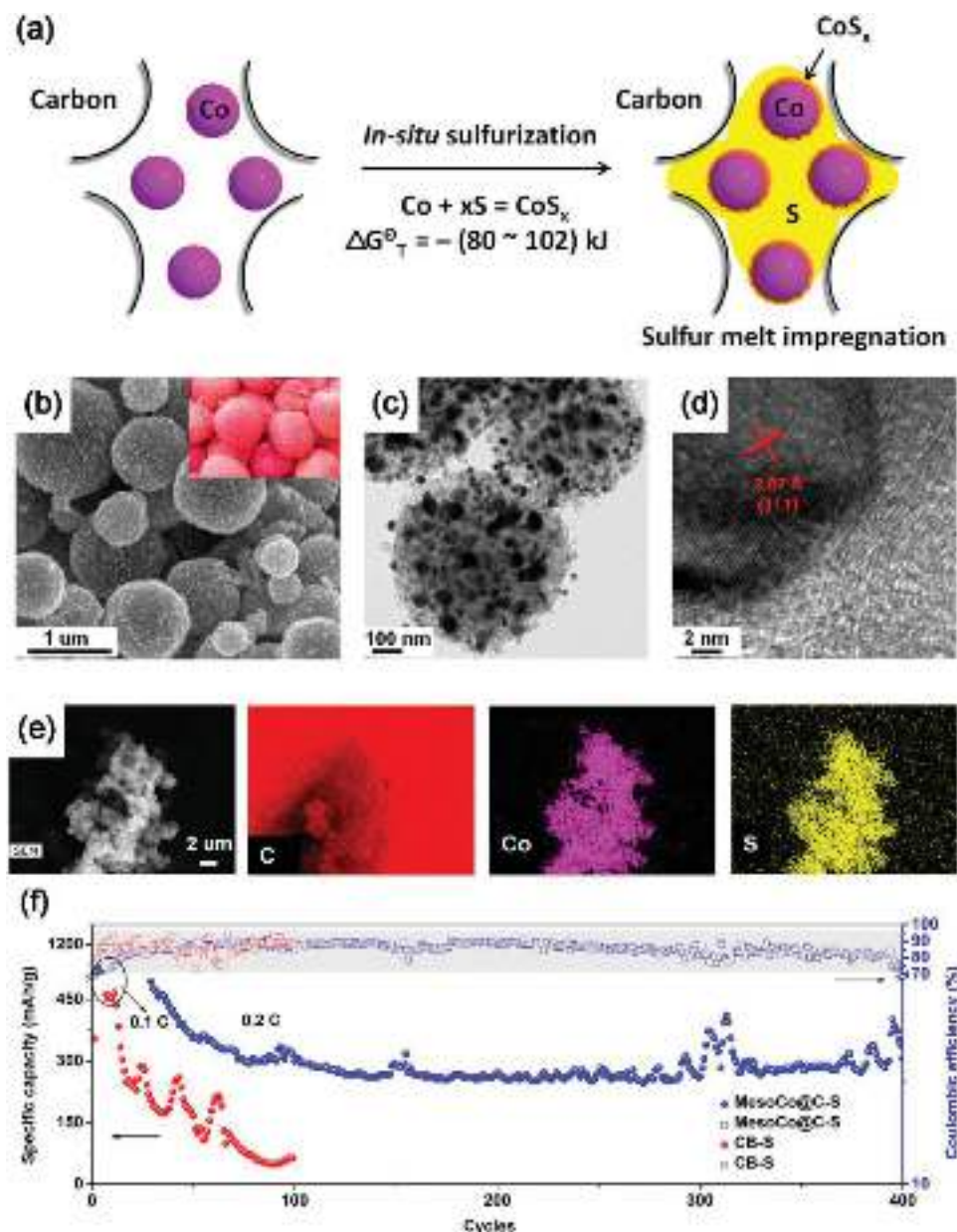


Figure 4. A carbon-confined sulfurized cobalt in a mesoporous matrix (MesoCo@C-S) as Mg-S cathode. a) Schematics of the in situ sulfurization of MesoCo@C precursor. b–d) Characterization of MesoCo@C precursor: b) SEM, c) TEM, d) HRTEM, and e) EDS images. Inset picture in (b) is a digital photo of lychee fruits for comparison. f) Comparison of long cycling stability and Coulombic efficiency between the MesoCo@C-S cathode and a carbon black cathode (CB-S). Reproduced with permission.^[22] Copyright 2020, American Chemical Society.

3.1.4. SGDY

In 2017, Du et al. developed a sulfur cathode based on SGDY which is compatible with nucleophilic electrolytes.^[17c] Graphdiyne has large interlayer distance (0.365 nm) and uniform pores (5.42 Å) within each layer. The highly reactive carbon–carbon triple bonds in graphdiyne can readily react with short sulfur species using a simple thermal synthesis at 350 °C. After reaction, the morphology of SGDY did not change while the short chain sulfur (S_n , $1 \leq n \leq 4$) was uniformly distributed in the pores of graphdiyne with a high content of 26.11 wt%. The Mg–S battery using SGDY cathode and nucleophilic all-phenyl

complex (APC) electrolyte with addition of LiCl showed a high initial discharge capacity of 1125 mAh g^{−1} and a capacity retention of 459 mAh g^{−1} after 36 cycles. The SGDY cathodes displayed almost no capacity without LiCl additive, which is explained by the absence of transformation of inactive MgS and MgS₂ to active Li₂S and Li₂S₂ by the Li ions.

3.2. Strategies Toward High-Performance S-Based Cathodes

Although various cathodes have been developed and tested for Mg–S batteries, current cathodes face many roadblocks on the

way to practical Mg–S batteries. For example, Mg–S cathodes often suffer a large overpotential, rapid capacity fading, and poor cycling efficiency.^[14a,16] These issues are directly related to the irreversible loss of sulfur active substances caused by the dissolution of sulfur and polysulfides from cathodes into the electrolyte and their subsequent shuttling to the anode, plus the sluggish kinetics of the reaction between Mg with sulfur. Unfortunately, under high sulfur conditions which are required by practical applications, these issues will be amplified and become more serious.^[19] To solve these problems, it is necessary to confine sulfur and polysulfides within the cathode region, and to improve the kinetics of the Mg–S reaction, making polysulfides, especially short-chain magnesium polysulfides with low solubility in the electrolyte, more easily oxidized to sulfur. Strategies related to cathode design to address the shuttle effect in Li–S batteries, such as forming covalent bonds between sulfur and carbon substrate and adding a protective layer on the cathode, can be adopted by Mg–S batteries.^[23] In addition, separator modification, thiophilic current collector selection (e.g., Cu), and electrolyte optimization in terms of the solvent viscosity and salt concentration, are also effective in suppressing the loss of active sulfur species.^[19,24]

4. Mg Anodes

Mg metal as an anode has many advantages including low cost, high capacity, and relatively low reduction potential. More importantly, unlike Li metal, Mg does not form dendrites upon cycling, eliminating safety concerns. Unfortunately, the commonly used carbonate-based solvents are incompatible with Mg metal due to

the formation of an impermeable layer on top of Mg. Therefore, new electrolytes that are compatible with both Mg and sulfur must be developed. Moreover, a solid layer is usually formed on Mg anodes via electrolyte decomposition or reaction with traces of water or oxygen, rendering Mg anodes with very high impedance (hundreds to thousands Ω) due to the sluggish Mg^{2+} ion transport through them.^[25] In fact, Mg anodes, with much higher impedance than sulfur cathodes, dominate the Mg–S battery impedance.^[14a] Therefore, the solid layer on Mg anode surface is the main challenge for practical application of Mg metal anodes. To enhance Mg anode plating/stripping performance, solid layers on Mg anodes should be prevented or modified to improve Mg^{2+} transport. Connell et al. found that trace amount of H_2O (≤ 3 ppm) in MgTFSI_2 /diglyme electrolyte slows the deposition kinetics of Mg^{2+} via strong solvation effect of H_2O , while a passivation layer (i.e., MgO and $\text{Mg}(\text{OH})_2$) forms only after Mg deposition ceases.^[26] They also revealed that adding Cl^- ions dramatically enhanced the reversibility of Mg deposition as Cl^- ions could protect the Mg surface from passivation by H_2O via the formation of adsorbed Cl^- (Mg-Cl^*) and/or MgCl_2 .

In Mg batteries, the surface film formed by electrolyte decomposition on Mg anodes can be passivation layer or SEI layer. The differences between them lie in their ability for Mg^{2+} ion transportation. Specifically, a passivation layer on Mg anodes impedes Mg^{2+} ion migration, while SEI layer allows the conduction of Mg^{2+} ions. Gao et al. reported the presence of SEI layer at the Mg/electrolyte interface that conducts Mg^{2+} ions under the driving force of a mild overpotential (see Figure 5a–d for further details).^[27] The authors studied Mg anodes in Mg–S batteries in an MgTFSI_2 – MgCl_2 electrolyte with different concentrations (from 0.25 to 1.2 M based on

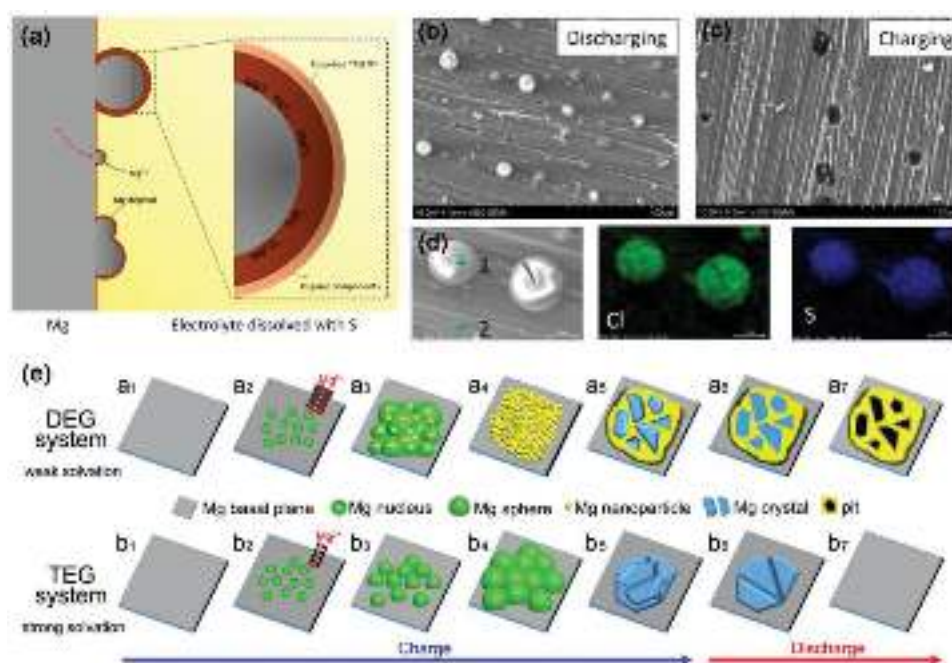


Figure 5. a) Structure of SEI on a Mg anode cycled in a sulfur containing MgTFSI_2 – MgCl_2 electrolyte. Morphology of Mg anode after discharging b) and charging c). d) EDX imaging of Mg anode after discharging in sulfur-containing electrolyte. Point 1: Mg deposits. Point 2: Mg substrate. Reproduced with permission.^[27] Copyright 2018, American Chemical Society. e) Schematic illustration of interfacial evolution of Mg anodes upon charging/discharging in DEG (a1–a7) and TEG (b1–b7) electrolytes. Reproduced with permission.^[30] Copyright 2018, Elsevier.

Mg(TFSI)₂), in terms of their electrochemistry and surface chemistry. A solid surface layer forms on the Mg/electrolyte interface through the reduction of electrolyte by Mg metal and it stops growing when the layer is thick enough to block electron transport. Mg²⁺ ions, however, can still migrate across the layer when a negative potential is applied to the Mg anode. When its ion conductivity is higher than electrical conductivity, the layer functions as a SEI and only a small overpotential is needed, as reported in some electrolytes.^[28] Otherwise, the solid layer functions as a passivation layer (e.g., in PC or AN-based electrolytes), resulting in a large overpotential.^[29] By analyzing this SEI layer using energy dispersive X-ray spectra (EDX) and XPS, a structure consisting of three layers was revealed, including 1) an inorganic layer of Mg compounds; 2) a middle organic compounds layer; and 3) an adsorptive TFSI⁻/Cl⁻ layer.^[27]

In 2018, Hu et al. observed interface changes on Mg anodes during plating/stripping in two different electrolyte solvents (i.e., DEG and TEG) based on a (HMDS)₂Mg–MgCl₂–AlCl₃ electrolyte using in situ atomic force microscopy.^[30] In DEG electrolyte (see Figure 5e(a1–a7)), amorphous bowl-like nuclei form at –0.26 V in the deposition process, then grow rapidly to spherical structures at a rate of ≈564 nm min⁻¹. After 8 min, cuboid shaped crystals with hexagonal-close-packed Mg crystal structure emerge and grow rapidly. During discharging in DEG electrolyte, regular crystals strip faster than the adjacent amorphous parts, resulting in pits formed on these crystals positions at –0.12 V after 12 min. In TEG electrolyte (see Figure 5e(b1–b7)), Mg nuclei starts to form at –0.48 V, and then grow into spherical structures with time at a rate of ≈197 nm min⁻¹ before finally combining together. The striping in TEG electrolyte shows slow interfacial dynamic processes. No Mg dendrite was found during charging in either DEG or TEG electrolytes. The different plating/stripping behaviors in DEG and TEG electrolytes were explained by different solvation and stabilization ability of the two solvents. The TEG molecule with five oxygen atoms can form a more stable chelating structure with [Mg₂(μ-Cl)₃]⁺ cations, leading to a lower conductivity (DEG electrolyte: 0.98 mS cm⁻¹; TEG electrolyte: 0.23 mS cm⁻¹) and a slower surface dynamics.^[31] This slow surface dynamics in TEG electrolyte allows uniform nucleation, crystallization, and stripping, thereby resulting in a higher specific capacity and better reversibility in Mg–S batteries.^[24c]

Tuerxun et al. attribute the reversible deposition of Mg in simple salt electrolytes (i.e., a commercial Mg salt dissolved in a solvent) to the coordination of structure between Mg ions and solvent molecules by investigating the polarization behavior of Mg anode using both experimental (i.e., in operando soft X-ray absorption spectroscopy (operando SXAS) and Raman) and computation methods (i.e., density functional theory (DFT)). Raman spectroscopy studies show that the coordination of electrolyte anions to Mg²⁺ ions is affected by solvent through competing solvation (i.e., solvent coordinating to Mg ions). For example, [TFSI]⁻ in 2-MeTHF solvent and [BH₄]⁻ in tetrahydrofuran (THF) solvent coordinated to Mg²⁺ ions while [TFSI]⁻ in triglyme solvent does not coordinate to Mg²⁺ ions. The coordination of solvent molecules to Mg²⁺ ions reduces their lowest unoccupied molecular orbital (LUMO) energy levels compared to uncoordinated solvent molecules according to DFT calculations. When the LUMO energy decreases to below the reduction potential of Mg²⁺ ions, these coordinated anions

will be preferentially reduced to release F⁻ and O²⁻ ions, which will react with Mg²⁺ ions to form a passivation layer on Mg anodes. For example, the Mg²⁺ ions strongly bound to [TFSI]⁻ in Mg(TFSI)₂/2-MeTHF electrolyte are prone to undergo reductive decomposition, rather than Mg depositing on metallic Mg anodes, which would imply the electrolyte is electrochemically inactive. In contrast, Mg²⁺ ions weakly bound by [TFSI]⁻ in Mg(TFSI)₂/triglyme electrolyte undergo slow reduction decomposition, allowing Mg to deposit on the anode.^[32]

Some *p*-block elements (e.g., In, Sn, Sb, Pb, and Bi) can reversibly form electrochemical alloys with Mg.^[33] This concept has been employed to prepare Mg-based anode in full cells matching with various cathodes, such as vanadium oxides, Chevrel phases, and Prussian blue analogues.^[34] The advantage of Mg alloy anodes relies on their compatibility with simple salt Mg electrolytes and their low air sensitivity. Very recently, Meng et al. introduced this concept to Mg–S batteries using a simple Mg(TFSI)₂/dimethoxy ethane (DME) electrolyte.^[35] By replacing Mg metal anodes with Mg₃Bi₂ alloy, the obtained Mg–S battery shows promising cycling performance at elevated current density.

5. Electrolytes

5.1. Basic Understanding of Mg Electrolytes

The electrolyte, functioning as an ion conducting medium between two electrodes, is a vital component in a metal–S system as it not only affects the dissolution of polysulfides on cathodes, but also determines the structure of the SEI on anodes. Specific to the Mg–S system, due to some unique properties of Mg metal (e.g., Mg can react with esters), some established knowledge of electrolytes in alkali metal–sulfur systems cannot be directly applied to the Mg–S system. For example, some simple lithium salts (e.g., LiPF₆) have achieved great success in lithium-based batteries. The Mg analogues of these Li salts, however, such as Mg((PF₆)₂) and Mg(ClO₄)₂ can be reduced to form an impermeable passivation layer on the surface of Mg anode which inhibits the migration of Mg ions to a Mg electrode surface.^[36] Therefore, developing reversible, sulfur-compatible electrolytes with favorable electrochemical properties is the main challenge facing Mg–S batteries in the current stage.

According to a previous survey, electrolytes are the most studied subject among all Mg–S battery components (i.e., cathodes, anodes, electrolytes, and separators).^[9a] The ideal electrolyte should have a number of key properties, including a wide electrochemical window, high chemical and electrochemical stability, high ionic conductivity, high thermal stability, and low toxicity and flammability.^[24c] In addition, the electrolyte should be kinetically stable to support reversible Mg²⁺ ion transport at the Mg/electrolyte interface without forming an impermeable blocking film, or any soluble reaction products that leads to electrolyte consumption. To meet these requirements, Mg electrolytes that are composed of solutes (i.e., the salts consisting of Mg-containing cations and Mg-free anions), solvents (e.g., ether and ionic liquids), and additives (e.g., LiCl) need to be carefully formulated.

The composition and performance of known and available electrolytes for Mg–S are summarized in **Table 2**. Organomagnesium-based electrolytes are commonly synthesized

Table 2. Summary of known Mg–S electrolytes.

Category	Feature	Name	Active component	Synthesis method	Anodic stability [V vs Mg] on Pt	CE [%]	Ionic conductivity [ms cm ⁻¹]	Ref
Nucleophilic organomagnesium-based electrolyte	1) Incompatible with sulfur; 2) Requires design of other battery components; 3) Cation can be only dissolved in THF	Dichloro complex (DCC)	[Mg ₂ (μ-Cl) ₃ ·6THF][RAlCl _n]	Transmetalation reaction between MgR ₂ (R = ethyl and butyl) and aluminum Lewis acid (e.g., AlCl ₃ , AlEtCl ₂ , etc.) in THF	2.2	100	1.4	[39]
		All phenyl complex (APC)	[Mg ₂ (μ-Cl) ₃ ·6THF]PhnAlCl _{4-n}	Transmetalation reaction between phenylmagnesium chloride (PhMgCl) and AlCl ₃ in THF	3.2	≈100%	5	[42]
Non/less-nucleophilic organomagnesium-based electrolyte	Amide-based: 1) Compatible with sulfur; 2) Sensitive to moisture and air	Amide-based electrolyte (HMDS-based)	[Mg ₂ (μ-Cl) ₃ ·6THF][HMDSAICl ₃]	Transmetalation reaction between HMDSMgCl and AlCl ₃ in THF	3.2	95–100	No data	[17a]
		Amide-based electrolyte (HMDS-based)	[Mg ₂ (μ-Cl) ₃ ·6THF][HMDSAICl ₃]	(HMDS) ₂ Mg·AlCl ₃ ·MgCl ₂ electrolyte by adding a LiTFSI additive in diglyme	≈2.7	92%	No data	[45]
		Amide-based electrolyte (HMDS-based)	[Mg(DG) ₂][HMDSAICl ₃] ₂	Pre-treatment of Mg[HMDS] ₂ using DG as the coordinating agent before reaction with AlCl ₃ in DG	3.5	≈100	No data	[46]
	Alkoxide-based: 1) Compatible with sulfur; 2) Insensitive to air and moisture	Magnesium bis(diisopropyl) amide (MBA)-based	[Mg ₂ (μ-Cl) ₃ ·6THF][AlCl ₄]	Reaction between MBA and AlCl ₃ in THF	2.65 V on SS electrode	≈100	0.947	[47]
		Magnesium bis(diisopropyl) amide (MBA)-based	[(C ₃ H ₇) ₂ N]MgCl ₂ ·MgCl	Reaction between MBA and MgCl ₂ in mixed solvents	No data	98	0.471	[48]
		Alkoxide-based electrolyte	ROMgCl·AlCl ₃	Reaction of Phenols (i.e., ROH) and Grignard reagent (i.e., EtMgCl), then addition of AlCl ₃ ·THF to form ROMgCl·AlCl ₃ ·THF electrolyte,	2.6	99	2.56	[49]
		Fluorinated alkoxyborate based	Mg[B(hfp) ₄] ₂	Reaction of Mg(BH ₄) ₂ with various fluorinated alcohols (RFOH) in diglyme (DEG) and tetraglyme (TEG)	3.5	>98	6.8	[51]
		Organic magnesium borate-based (OMBB)	[Mg ₄ Cl ₆ (DME) ₆][B(HFP) ₄] ₂	In situ reaction of tris(hexafluoroisopropyl) borate [B(HFP) ₃], MgCl ₂ and Mg powder in 1,2-dimethoxyethane (DME).	3.3	98	5.58	[54]
		Boron-centered anion-based magnesium (BCM)	[Mg(DME) _n][FTHB] ₂	Reaction of MgF ₂ with THFPB in DME	3.5	99.8	1.1	[53]
		Weakly coordinating anions (WCAs)-based	Mg[B(hfp) ₄] ₂ /DME (hfp = OC(H)(CF ₃) ₂)	Reaction of Mg(BH ₄) ₂ with several fluorinated alcohols (RFOH) in ethereal solvents	3.5	98	6.8	[51]
	Boron-based: 1) Noncorrosive; 2) Easy dissociation of organoborate anions; 3) Functionality of groups grafted on the boron center atom							

Table 2. Continued.

Category	Feature	Name	Active component	Synthesis method	Anodic stability [V vs Mg] on Pt	CE [%]	Ionic conductivity [mS cm ⁻¹]	Ref
All-inorganic electrolyte	1) Nonnucleophilic; 2) Chemical and anodic stable; 3) Cost-effective; 4) Readily synthesizable; 5) MACC electrolyte requires a conditioning procedure	Inorganic magnesium aluminum chloride complex, MACC	$Mg_{(m)}Al_{(n)}Cl_{[(2^m)+(3^n)]}$	Reaction of $MgCl_2$ and $AlCl_3$ in ethereal solutions, such as THF, DME, and tetraglyme	3.1	99	2	[1b]
		MACC	$[Mg(THF)_6]^{2+}$ cation and $[AlCl_4]^-$	Simply heating $MgCl_2$ and $AlCl_3$ in the mixed solution of THF and an ionic liquid $PYR_{44}TFSI$.	2.5	≈100	8.5	[60]
simple salt electrolyte	1) Commercially available; 2) Better sulfur compatibility; 3) High ionic conductivity; 4) High anodic stability	$MgCl_2$ - YCl_3 electrolyte [R56]	No report	Reaction of $MgCl_2$, YCl_3 , $AlCl_3$, and $PYR_{44}TFSI$ in DG	3	≈98.7%	No data	[17b]
		Simple salt electrolyte	$Mg(TFSI)_2$	$Mg(TFSI)_2$ dissolved in glyme/diglyme	3 on SS	96.1	3.03	[61]
		Concentrated simple salt electrolyte	$Mg(TFSI)_2$ - $MgCl_2$ -DME electrolyte	By simply dissolving commercial Mg salts in DME	3	93	No data	[24b]
		$Mg(CF_3SO_3)_2$ - $MgCl_2$ - $AlCl_3$ electrolyte	$[Mg_2(\mu-Cl)_2(DME)_4][AlCl_3(CF_3SO_3)]$	Dissolving $Mg(CF_3SO_3)_2$ - $MgCl_2$ - $AlCl_3$ electrolyte in DME	3.5	99.1	No data	[67b]

by transmetalation reactions between an organomagnesium Lewis base with an aluminum- or boron-centered Lewis acid. Therefore, Organomagnesium-based electrolytes can be categorized into different types, such as nucleophilic organomagnesium (e.g., $RMgX$ and MgR_2 , R = alkyl, aryl groups and X = Cl, Br), and non-nucleophilic organomagnesium electrolytes including amide-based (e.g., $(HMDS)_2Mg$ and magnesium bis(diiisopropyl)amide (MBA)), and alkoxide-based (e.g., $ROMgX$) electrolytes according to the initial form of organomagnesium precursors (e.g., $R-Mg$, $RN-Mg$, and $RO-Mg$). In this section, a comprehensive overview with thorough discussion on the developed Mg electrolytes in terms of various Mg salts (based on organomagnesium salts, all-inorganic salts and simple salts) and solvents is provided. In addition, strategies confronting the corrosivity of designed Mg electrolytes to the metallic components in batteries are also reviewed.

5.2. Design Strategies for Mg Electrolytes

5.2.1. Organomagnesium Salt-Based Electrolytes

Cation Design: Nucleophilic Organomagnesium Salt-Based Electrolytes: It is well known that Mg shows a reversible deposition and dissolution behavior in ether solutions of Grignard reagents ($RMgX$, R = alkyl, aryl groups and X = Cl, Br).^[37] Such solutions, however, cannot be used in Mg batteries due to intrinsically strong nucleophilic and reducing R groups, which leads to a narrow electrochemical window (<1.8 V vs Mg/Mg^{2+} on Pt). In 1990, Gregory et al. first synthesized electrochemically active Mg electrolytes beyond Grignard reagents through the reaction of alkyl Grignard reagents with Lewis acids (e.g., $AlCl_3$ or trialkylborane) in tetrahydrofuran (THF).^[38] In 2000, Aurbach et al. further refined the Mg electrolyte formulation by adjusting the ratio of MgR_2 (R = ethyl and butyl) to aluminum Lewis acid (e.g., $AlCl_3$, $AlEtCl_2$, etc.) and demonstrated the first prototype rechargeable Mg battery.^[39] This electrolyte, also called dichloro complex (DCC), exhibited a high ionic conductivity of 1.4 mS cm⁻¹, a high oxidative stability of 2.2 V versus Mg and a high CE of 100%.^[39] As the DCC electrolyte is generated through an in situ transmetalation reaction, its electrochemical properties depend mainly on equilibrium species in the electrolyte in which ligand exchange of inorganic and organic ligands occurs rapidly between the Mg and Al cores.^[40] The relatively weak aluminum–carbon bond in DCC electrolyte tends to break via β -hydrogen-elimination upon electrochemical cycling, which limits the oxidative stability of DCC electrolyte.^[41]

To improve the oxidative stability of DCCs, the second generation of electrolytes, referred to as “all phenyl complexes” (APC), were developed by a reaction between phenylmagnesium chloride ($PhMgCl$) and $AlCl_3$. The substitution of alkyl groups into the organomagnesium precursor of DCC with aromatic groups without β -hydrogen endows APC electrolytes with an oxidative stability of 3.2 V versus Mg, a conductivity of 5 mS cm⁻¹ (30 °C) and a CE of almost 100%.^[42] Crystallizing the electrolyte by precipitation upon addition of hexane allowed the researchers to characterize the structure of Mg electrolyte. Both DCC and APC electrolytes contain Mg dimer cations

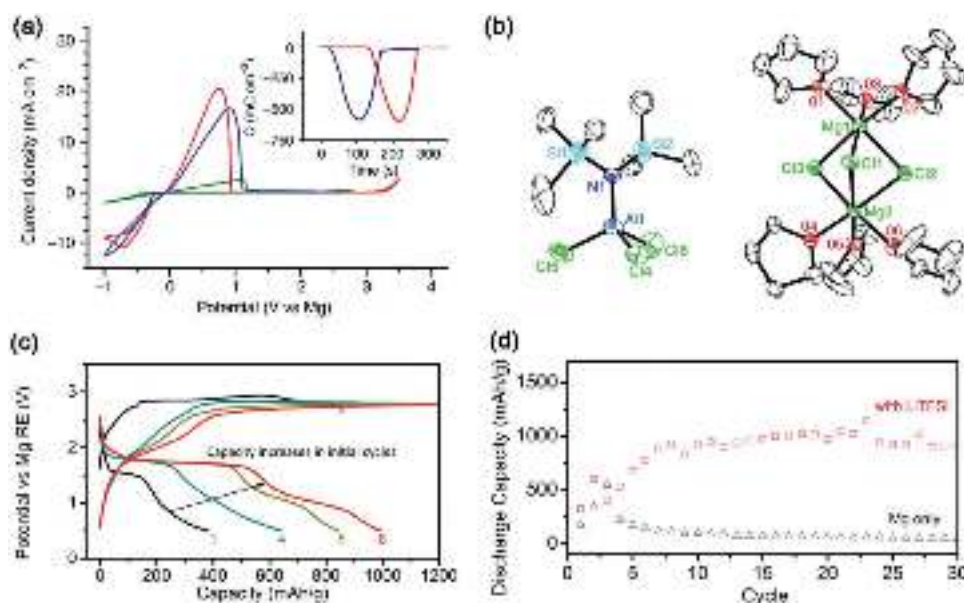


Figure 6. Structure and performance of Amide-based electrolyte prepared using HMDSMgCl. a) Cyclic voltammograms of HMDSMgCl (green), an in situ mixture of HMDSMgCl to AlCl_3 (blue), and the crystal obtained from a mixture of HMDSMgCl to AlCl_3 (red). Inset shows the charge balance during Mg deposition/dissolution. b) Structure of the crystallized product from the mixture of HMDSMgCl with AlCl_3 . Reproduced with permission.^[17a] Copyright 2011, Nature Publishing Group. c) Charge/discharge curves of a sulfur cathode in 0.1 M Mg-HMDS electrolyte with 1.0 M LiTFSI. d) Cycling stability in electrolyte with and without LiTFSI. Reproduced with permission.^[45] Copyright 2015, American Chemical Society.

(i.e., $[\text{Mg}_2(\mu\text{-Cl})_3 \cdot 6\text{THF}]^+$) and aluminate anions (e.g., AlCl_4^- and $\text{Ph}_n\text{AlCl}_{4-n}$).^[42a,43]

These in situ generated organomagnesium salt-based electrolytes (i.e., DCC and APC) from the reaction between a Lewis base and a Lewis acid constitute a complex, chemical species in dynamically equilibrium with highly nucleophilic components (RMgX and MgR_2) in the ether solvent. Although they can be directly used in rechargeable Mg ion batteries and display good electrochemical performance, their nucleophilicity makes them incompatible with electrophilic sulfur cathodes. Nonetheless, recent research work has proved that by selecting a suitable current collector^[19,20] and/or designing a new sulfur-based cathode,^[17c] Mg-S batteries based on nucleophilic APC electrolyte can be cycled successfully. In 2017, Zeng et al. used Cu current collectors to replace stainless steel (SS) current collectors, to construct APC electrolyte-based Mg-S batteries. They declared that the copper sulfide formed on the sulfur electrode/Cu current collector interface during the heating and drying process could protect sulfur and increase its compatibility with the APC electrolyte. The obtained Mg-S battery exhibited an initial discharge capacity of 659 mAh g^{-1} , and a capacity retention of 113 mAh g^{-1} after 20 cycles, indicating feasibility of APC electrolyte-based Mg-S batteries.^[20] In addition to forming a protective copper sulfide layer, other sulfur cathode designs (such as sulfur@sulfide graphite diyne (SGDY) and sulfur @microporous carbon cathodes) with the introduction of short sulfide species could also reduce the electrophilicity of sulfur, and improve sulfur compatibility with nucleophilic APC electrolyte.^[17c,19]

Non/Less-Nucleophilic Organomagnesium Salt-Based Electrolytes: Despite some reports on Mg-S batteries with nucleophilic electrolytes, intrinsically, these nucleophilic electrolytes are

not compatible with electrophilic S, between which reaction occurs and disulfide/sulfide forms. Against this backdrop, non/less-nucleophilic electrolytes have been extensively developed and applied as mainstream electrolytes for Mg-S batteries. Non/less-nucleophilic electrolytes are generally synthesized by reactions between a non-nucleophilic Mg-containing Lewis base and a Lewis acid. In non/less-nucleophilic bases, Mg is bonded with N or O rather than C which forms nucleophilic C-Mg bonds. The commonly used non/less-nucleophilic bases include amide-based organomagnesium (i.e., RNMg) and alkoxide-based organomagnesium (ROMgCl), while Lewis acid includes aluminum- and boron-centered Lewis acids.

Amide-Based Electrolytes: In 2000, Liebenow et al. reported reversible Mg plating and stripping in an electrolyte based on non-nucleophilic Hauser base hexamethyldisilazide magnesium chloride (HMDSMgCl). Its performance, however, such as Coulombic efficiency, voltage stability, and current density are inferior to the organohaloaluminate electrolyte.^[44] In 2011, Muldoon et al. improved the electrochemical performance of HMDSMgCl by adding AlCl_3 to the solution.^[17a] By adding AlCl_3 , the current density for Mg deposition of the HMDSMgCl electrolyte was increased almost sevenfold (Figure 6a). The reaction product of HMDSMgCl and AlCl_3 was $[\text{Mg}_2(\mu\text{-Cl})_3 \cdot 6\text{THF}]^+ [\text{HMDSAlCl}_3]^-$ confirmed by single-crystal X-ray diffraction. Its structure is as shown in Figure 6b. The two octahedrally coordinated Mg atoms in the center are bridged by three Cl atoms while THF molecules are coordinated to the three remaining sites on each Mg via oxygens. The cation of DCC and APC electrolyte is also this $[\text{Mg}_2(\mu\text{-Cl})_3 \cdot 6\text{THF}]^+$ cation.^[42a,43] By crystallizing the electrolyte generated in situ and redissolving the crystals, any unreacted HMDSMgCl that starts to electrochemically oxidize and decompose around a voltage of 2.5 V can be

removed, leading to enhanced electrochemical performance. For example, the voltage stability was increased to 3.2 V and the Coulombic efficiency was improved from 95% to 100% for the re-dissolved electrolyte.^[17a] This purification method is also used for other electrolytes generated in situ such as DCC, APC and magnesium aluminum chloride complex (MACC). Using bisamide-based, non-nucleophilic electrolyte, Muldoon et al. reported the first rechargeable Mg-S battery with the initial discharge capacity of 1200 mAh g⁻¹. The second discharge capacity, however, dropped to 394 mAh g⁻¹ due to sulfur dissolution and polysulfide shuttling.^[17a]

It is noted that the electrochemically active product [Mg₂(μ-Cl)₃·6THF][HMDSAICl₃] can be obtained in THF only, which limits the choices of solvents for adjusting the physicochemical properties of the electrolyte. Against this backdrop, Zhao-Karger et al. developed amide-based electrolyte in mixed ethereal solvents (i.e., diglyme and tetraglyme) with ionic liquid as additive.^[24c] The authors used a one-pot, two-step method to form the active product [Mg₂Cl₂][HMDSAICl₃] by sequentially adding AlCl₃ and MgCl₂ into (HMDS)₂Mg ether solution. The Mg-S battery using this electrolyte showed an initial discharge capacity of 550 and 250 mAh g⁻¹ after 20 cycles. By adding ionic liquid (i.e., PP14TFSI) as an additive, the capacity was increased to 800 and 280 mAh g⁻¹ at 1st and 20th cycle, respectively. The addition of ionic liquid with high viscosity and weakly coordinating TFSI⁻ anions impeded the dissolution and diffusion of polysulfides, thereby improving the capacity retention rate. The oxidation stability, however, was reduced to about 3 V due to impurities in the ionic liquid.^[24c] Gao et al. further enhanced the reversibility of Mg-S batteries based on (HMDS)₂Mg-AlCl₃-MgCl₂ electrolyte by adding a LiTFSI additive (see details in Figure 6c,d).^[45] The resulting Mg-S battery with LiTFSI delivered a highly stable discharge capacity of 1000 mA h g⁻¹ for 30 cycles. The enhanced properties were attributed to 1) Li⁺ may participate in the cathode reaction to form readily rechargeable Li polysulfide (Li-PS) and 2) Li⁺ can coordinate to lower order Mg polysulfide, therefore increasing its solubility, reducing its reoxidation energy barrier and making it electrochemically active.^[45]

Although dimer Mg cations are popular in Mg electrolytes (including DCC, APC, and amide-based electrolyte), their large size is unfavorable for ion migration. Therefore, it is important to develop simple-type Mg salts as efficient Mg-S battery electrolytes. Direct reaction between organomagnesium salts and AlCl₃ unavoidably forms dimer Mg cation [Mg₂(μ-Cl)₃]⁺. To form a simple-type Mg ion, a Mg precursor needs to be pre-coordinated to prevent Mg-Cl bond formation. Xu et al. proposed a pretreatment of Mg[HMDS]₂ using DG as the coordinating agent to form stable cation [Mg(DG)₂]²⁺ before reaction with AlCl₃.^[46] The structure of the obtained electrolyte is characterized as [Mg(DG)₂][HMDSAICl₃]₂. The concentration of [Mg(DG)₂][HMDSAICl₃]₂ salt in DG solvent can reach above 1 M. The oxidative stability is 3.5 V on Pt electrodes and ≈3.0 V on stainless steel electrode. The lower oxidative potential on stainless steel electrode could presumably be due to the corrosion by Cl species in the electrolyte. The assembled Mg-S batteries showed a capacity of 400 mA h g⁻¹ after 100 cycles.^[46]

In 2019, Zhao et al. reported a new class of amide-based non-nucleophilic electrolyte for Mg-S batteries through a reaction of magnesium bis(diisopropyl)amide (MBA) and

AlCl₃.^[47] The active specie of this electrolyte was confirmed as [Mg₂(μ-Cl)₃·6THF][AlCl₄] by single-crystal X-ray diffraction. For Mg plating/stripping process, this MBA-based electrolyte showed high oxidative stability on stainless steel (2.65 V, vs Mg), low overpotential and close to 100% Coulombic efficiency. By including LiCl as an additive, assembled Mg-S batteries showed stable capacity of ≈540 mAh g⁻¹ up to 30 cycles.^[47] Later, Yang et al. used MgCl₂ instead of AlCl₃ to react with commercially available MBA in THF solvent under an inert atmosphere to form a new MBA-MgCl₂ electrolyte.^[48] The optimized MBA-MgCl₂ electrolyte by adjusting the ratio between MgCl₂ and MBA displayed an over-potential of 0.2 V, a Coulombic efficiency of 98% and a high ionic conductivity of 471 μS cm⁻¹. The authors also studied the performance of MBA-MgCl₂ electrolyte in a binary solvent of THF mixed with TG or DME and noted the effects of AlCl₃ adding into MBA-MgCl₂ electrolytes. The stability of MBA-MgCl₂ electrolyte depends on the oxidation of N-Mg bonds that can give electrons at sufficiently high potentials. Addition of strong Lewis acid AlCl₃ with high electron affinity can stabilize the N-Mg bonds by forming strong interactions between AlCl₃ and N-Mg bonds. The Mg-S battery based on the MBA-MgCl₂-AlCl₃ electrolyte demonstrated an initial discharge capacity of 1042 mAh g⁻¹ and a capacity retention of 276 mAh g⁻¹ after 20 cycles. After further addition of LiCl, the discharge capacity was increased to 1116.1 mA h for the first cycle and maintained 518 mA h g⁻¹ in the 80th cycle.^[48] This improvement can be attributed to the enhanced conductivity by adding Li⁺ and improved interfacial compatibility between the sulfur cathode and the electrolyte.^[47]

Alkoxide-Based Electrolytes: The less reactive alkoxide Mg salts (e.g., ROMgCl) that are insensitive to air and moisture have also been investigated as electrolytes for Mg rechargeable batteries. The alkoxide Mg salts are generally synthesized via a two-step method: 1) An oxygen-containing organic molecule reacts with a Grignard reagent to form ROMgCl salt; 2) then ROMgCl reacts with AlCl₃ in THF to form ROMgCl-AlCl₃-THF electrolyte. For example, in 2012, Wang et al. used three different phenols (i.e., ROH) to react with a Grignard reagent (i.e., EtMgCl), then AlCl₃-THF solution was added dropwise to each reaction solution to form ROMgCl-AlCl₃-THF electrolyte.^[49] One of these electrolytes (i.e., (BMPMC)₂-AlCl₃/THF) with high ionic conductivity (2.56 mS cm⁻¹) and oxidation stability (2.6 V vs Mg RE) displayed reversible Mg plating and stripping.

Later, Liao et al. prepared three alkoxide Mg electrolytes including *n*-BuOMgCl, *tert*-BuOMgCl, and Me₃SiOMgCl using an alcohol, aldehyde, and ketone as precursors (such as *tert*-butanol and silanol).^[50] All the three alkoxide Mg salts were nonpyrophoric and highly soluble in THF (up to 2 M). Their THF solutions displayed high ionic conductivities (e.g., 1.20 mS cm⁻¹ for 1.2 M *tert*-BuOMgCl/THF), good oxidation stabilities (1.8–2 V vs Mg/Mg²⁺) and reversible Mg deposition/stripping processes. Both ionic conductivity and oxidation stable voltage were further increased by adding AlCl₃. The authors also demonstrated good cycling and rate performance of these alkoxide-based Mg electrolytes in Mg-Mo₆S₈ batteries.^[50] Zhao-Karger et al. reported a fluorinated alkoxyborate based Mg electrolytes with a high anodic stability, ionic conductivity, and Coulombic efficiency for Mg deposition by the reaction of Mg(BH₄)₂ with various fluorinated alcohols (R^FOH) in ethereal

solvents.^[51] The authors tested their electrolyte in a Mg–S batteries using S/CMK-3 as the sulfur cathodes. Although undesired “electrolyte conditioning” (i.e., discharge capacity increases after 1st cycle) or/and the refreshment and activation of the Mg anode surface over cycling were observed, the Mg–S battery displayed a reversible discharge capacity of 200 mA h g^{−1} after 100 cycles, which indicates that the fluorinated alkoxyborate based Mg electrolytes are compatible with a sulfur cathode.^[51]

Anion Design: The anions of organomagnesium salt-based electrolytes are comprised of a high-valence central atom (i.e., B, Al, P, S, Cl, and As) surrounded by functional groups (such as −F, −Cl, −O, −OR etc.). Anions centered with Cl, P, and As elements including ClO₄[−], PF₆[−], and AsF₆[−] can be reduced by Mg metal, forming an passivation layer that impedes Mg²⁺ ion migration.^[52] Anions with S as the central atom can form simple salt electrolytes with Mg ions (e.g., Mg(CF₃SO₃)₂, Mg(TFSI)₂). While Al-centered anion (termed as “organohaloaluminate”) and B-centered anion (termed as “organoborate”) are the two main types of desirable anions, which promote reversible Mg deposition in electrolytes. Generally, the pioneering Mg electrolytes, including nucleophilic Grignard reagent-based electrolytes, non-nucleophilic amide-based electrolytes, and alkoxide-based electrolytes, are comprised of Al-centered anions. As these electrolytes contain the same dimer Mg cation, [Mg₂(μ-Cl)₃]⁺, their solubility and redox stability mainly depend on the involved anions.

In addition to Al-centered anions, B-centered anions, such as BH₄[−], [BBu₄][−], and [CB₁₁H₁₂][−], comprise numerous efficient Mg electrolytes that are compatible with Mg metal. The general formula of B-centered anions can be described as [BX_nY_{4−n}][−], where X is bridging group and Y is the terminal group. Different choices for X and Y can yield many different B-centered anions. The corrosive nature of Mg electrolytes comes from the chlorine-containing cation or anion.^[36a] For example, the chlorine in [Mg₂(μ-Cl)₃·6THF]⁺ cation, which can be found in all crystallized magnesium organohaloaluminate electrolyte, will lead to the corrosion of Mg anodes.^[36a] This phenomenon is also observed for most simple Mg salt electrolytes and all-inorganic Mg electrolytes with Cl in their anions. In contrast, B-centered anions in the developed Mg electrolytes are usually Cl free, which are considered as promising candidates for developing noncorrosive electrolytes. Characteristics for known anions with different central elements are depicted in **Figure 7a**.^[53] Notably, the solvated structures of cations and anions largely determine the electrochemical properties of Mg electrolytes by impacting numerous factors including their useful electrochemical window, ion conductivity, anodic stability, and compatibility with Mg anodes. Therefore, selecting and designing the cations and anions is an effective way to tailor the stability and conductivity of Mg electrolyte and much effort has been invested in this area.

Organic Magnesium Borate-Based Electrolytes: In 2017, Zhang et al. proposed the design principle of boron-centered anion-based magnesium (BCM) electrolytes (**Figure 7a–c**): 1) Large, monovalent and bulky organoborate anions are easily dissociated due to low lattice energy with cations; 2) Selecting functional groups grafted on the B central atom with high anodic stability can enlarge the electrochemical window of the resulting electrolyte. For example, they pointed out that

fluorinate terminals with powerful electron-withdrawing property could improve the thermal and electrochemical stability by tailoring the highest occupied molecular orbital condition of the anion.^[53] By adopting these design principles, the authors reported a BCM salt, which was composed of [Mg(DME)_n]²⁺ cations and large, bulky [FTHB][−] anions with electrochemically stable alkoxy bridging and −CF₃ terminating groups (**Figure 7a**). When employed in Mg electrolyte, it displayed all-round merits including facile synthesis, high CE (99.8%), high ionic conductivity (1.1 mS cm^{−1}), high anodic stability (i.e., 3.5 V) and noncorrosivity (**Figure 7b,c**). Notably, assembled Mg–S batteries exhibited high average discharge capacity up to 1081 mA h g^{−1} during the first 30 cycles with one flat voltage plateau of ≈1.1 V versus Mg (**Figure 7c**). Nevertheless, discoloration was observed in the BCM electrolyte after cycling due to dissolution of polysulfide, which implies the happening of polysulfide shuttling. To suppress the shuttle effect, the authors proposed to reduce the amount and increase the viscosity of the electrolyte.^[53]

Du et al. developed a new, non-nucleophilic Mg borate-based electrolyte (OMBB) for Mg–S battery (**Figure 7d**).^[54] The OMBB electrolyte was synthesized through *in situ* reaction of tris(hexafluoroisopropyl)borate [B(HFP)₃], MgCl₂, and Mg powder in DME. The equilibrium species in the electrolyte were determined to be [Mg₄Cl₆(DME)₆]²⁺ and [B(HFP)₄][−] by a series of characterization methods including NMR, mass spectroscopy and single-crystal X-ray powder diffraction. The larger tetranuclear [Mg₄Cl₆(DME)₆]²⁺ complex required less energy for desolvation during the Mg plating process compared to mononuclear [Mg(DME)₃]²⁺ cation, leading to higher Mg plating/stripping reversibility.^[55] The addition of MgCl₂ induced ligand exchange between Cl ions and DME solvent in the cation complex to form a more thermodynamically stable form. Moreover, the Cl ions also improved the stability of electrolytes by minimizing electrochemically inactive species. As a result, the as-prepared Mg electrolyte displayed a high ionic conductivity of 5.58 mS cm^{−1}, high anodic stability up to 3.3 V (vs Mg/Mg²⁺), high Coulombic efficiencies greater than 98% and a low overpotential of 0.11 V. When coupled with sulfur-carbon nanotubes (S-CNTs) cathodes, a highly reversible Mg–S battery for 100 cycles was constructed, showing a high discharge capacity of up to 1247 mA h g^{−1} and a maximum charging current rate 500 mA g^{−1} (**Figure 7e**).^[54]

Weakly Coordinating Anions-Based Electrolytes: B-centered molecules are also used to construct weakly coordinating anions (WCAs). The WCA compound has the formula of Mg[Z(OR^F)₄]₂, where Z = B, Al; R^F = fluorinated alkyl group. WCAs have unique advantages, such as low nucleophilicity, high ion conductivity, and high solubility.^[56] In 2017, Zhao-Karger et al. reported a series of WCAs-based Mg electrolytes comprising fluorinated alkoxyborates prepared by a reaction between Mg(BH₄)₂ and several fluorinated alcohols (R^FOH) in ethereal solvents.^[51] After the reaction, the solution was first dried to eliminate any excess fluorinated alcohol then the electrolyte was obtained by dissolving the dried solid in DME. The obtained 0.6 M Mg[B(hfp)₄]₂/DME (hfp = OC(H)(CF₃)₂) electrolyte showed a high conductivity of 6.8 mS cm^{−1}, a high Coulombic efficiency of >98% after 100 cycles and an anodic stability of ≈3.5 V on Pt and surprisingly high oxidative stability of 4.3 V on Al and stainless steel. This high oxidation stability was also observed in other studies, but was not explained

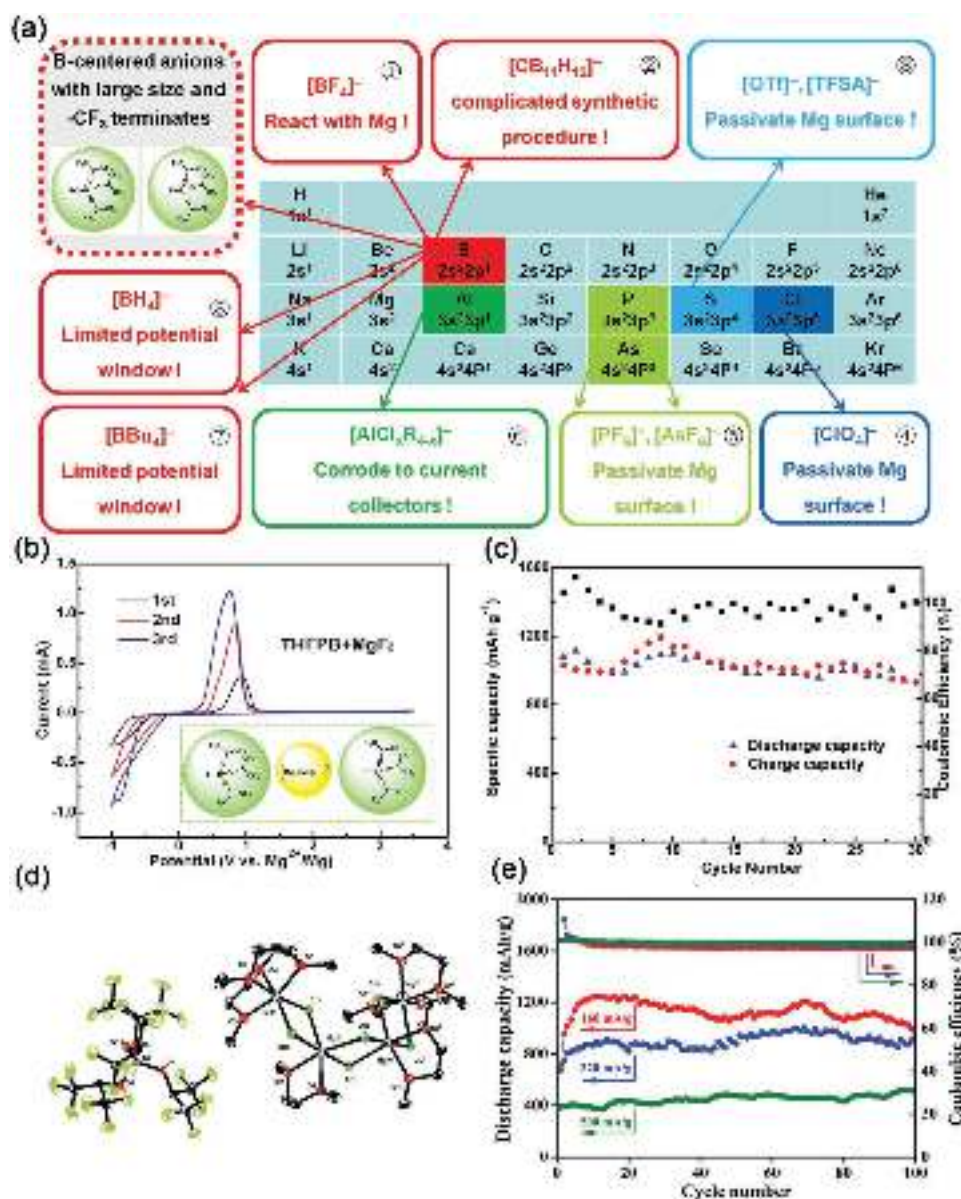


Figure 7. Anion design for Mg-S electrolytes. a) Decorated periodic table for guiding anion design for Mg electrolytes. b) CV curves of a sulfur cathode in a BCM electrolyte. The inset is the schematic structure of the Mg electrolyte. c) Cycling stability of the sulfur cathode in a coin cell containing BCM electrolyte. Reproduced with permission.^[53] Copyright 2017, Wiley-VCH. d) The molecular structure of [Mg₄Cl₆(DME)₆][B(HFP)₄]₂ crystal using the ORTEP plot. e) Discharge capacities and Coulombic efficiencies of the S-CNT cathode in the 0.5 M OMBB electrolyte at different current rates. Reproduced with permission.^[54] Copyright 2017, Royal Society of Chemistry.

satisfactorily.^[17c,32,51,57] Combined with S/CMK-3 cathodes, the resulting Mg-S batteries displayed a reversible discharge capacity of $\approx 200 \text{ mA h g}^{-1}$ after 100 cycles.^[51]

In 2018, the same group further investigated the concentration-dependent and electrode-dependent performance of Mg[B(hfp)₄]₂ electrolyte.^[58] Their results showed that the overpotential for Mg deposition decreases from -0.43 to -0.32 V as the electrolyte concentration was increased from 0.1 to 0.4 M . The electrolyte displayed lowest plating potential of -0.25 V on Cu electrodes and highest stability $>4.5 \text{ V}$ on Pt electrodes. The electrode-dependent performance could be due to the

different Mg nucleation energetics on surfaces of different electrodes. The conductivity of electrolyte increased first and then decreased with an increase of concentration, peaking at 0.3 M with a high conductivity of $\approx 11 \text{ mS cm}^{-1}$. Although 0.4 M electrolyte had lower conductivity, it outperformed 0.3 M electrolyte in Mg-S battery as the concentrated electrolyte inhibits the dissolution of polysulfides. Using 0.4 M Mg[B(hfp)₄]₂ electrolyte, binder-free activated carbon cloth/S cathode, and CNF-coated separator, the resultant Mg-S batteries achieved a reversible discharge capacity of about 660 mAh g^{-1} with a Coulombic efficiency close to 100% retained after 20 cycles.^[58]

5.2.2. All Inorganic Salt-Based Electrolytes

Although organometallic salt-based electrolytes have excellent reversibility, they are unstable to moisture and air and many of them are pyrophoric. To this end, inorganic Mg salt-based electrolyte, as another type of Mg electrolyte, has been developed. The inorganic Mg salt-based electrolytes are non-nucleophilic, chemical and anodic stable, cost-effective, and facile to be synthesized. In 2014, Doe et al. first reported a completely inorganic Mg electrolyte (i.e., inorganic, MACC) with highly reversible Mg deposition and large electrochemical stability through a reaction of MgCl_2 and AlCl_3 . The acid-base reaction is similar to the transmetalation reaction of Grignard reagent complexes for organometallic salt-based electrolytes. The solvents for the reaction can be a variety of ethereal solutions, such as THF, 1,2-dimethoxyethane (monoglyme, DME) and higher glymes, such as tetraglyme. In spite of an average cell overpotential of 200 mV, the electrolyte exhibited high anodic stability (i.e., 3.1 V vs Mg), high Mg ion conductivity ($\approx 2 \text{ mS cm}^{-1}$) and high Coulombic efficiency (i.e., $>98\%$).^[1b]

Generally, MACC electrolyte requires a conditioning procedure that is accompanied with irreversible Al decomposition at the working electrode and oxidation of Mg at the counter electrode to obtain efficient Mg electrodeposition and stripping with a high anodic stability window ($>3 \text{ V vs Mg/Mg}^{2+}$).^[59] To reduce the undesired need for conditioning, many methods have been developed. For example, increasing the concentration of MgCl_2 and AlCl_3 leads to a higher Mg electrodeposition current density, lower overpotential and much faster conditioning procedure.^[59b] Besides, adding a small concentration of $\text{Mg}(\text{HMDS})_2$ (i.e., $2\text{--}5 \times 10^{-3} \text{ M}$) can suppress Al^{3+} deposition and promote Mg electrodeposition and stripping from the first cycle.^[59a]

In 2016, Li et al. used an all-inorganic electrolyte for a Mg–S battery for the first time (details shown in Figure 8).^[60] They synthesized the all-inorganic electrolyte by simply heating MgCl_2 and AlCl_3 in a mixed solution of THF and PYR14TFSI ionic liquid. The ionic liquid was employed as a solvent to completely remove the Cl ions from MgCl_2 by the Lewis acid AlCl_3 . The electrochemically active species in the electrolyte were determined to be a simple Cl-free $[\text{Mg}(\text{THF})_6]^{2+}$ cations and $[\text{AlCl}_4]^-$ anions. In contrast to the $[\text{Mg}_2(\mu\text{-Cl})_3(\text{THF})_6]^{2+}$ cation that is formed in almost all the organohaloaluminate or organoborate electrolytes in THF solution, the $[\text{Mg}(\text{THF})_6]^{2+}$ is Cl-free and has a mononuclear Mg cation, which gives two advantages, namely: 1) the nonchlorinated cation can help solve the corrosion issue caused by Cl element; 2) the mononuclear Mg salt facilitates Mg^{2+} ion transport in the electrolytes and at the Mg/electrolyte interface. The electrolytes exhibited reversible Mg plating/stripping (>100 cycles), good anodic stability (2.5 V vs Mg), and high ionic conductivity (8.5 mS cm^{-1}). The resulting Mg–S battery showed an initial capacity of 700 mAh g^{-1} but dropped to about 100 mAh g^{-1} by the 20th cycle.^[60] The surface layer on the Mg/electrolyte was improved in this electrolyte while the polysulfide dissolution issue still existed. Very recently, the same group further improved the performance of Mg–S batteries with a new type of all-inorganic electrolyte: $\text{MgCl}_2\text{-YCl}_3$ electrolyte.^[17b] The low standard electrode potential of Y (i.e., -2.372 V) prevents its deposition during Mg plating,

thereby avoiding the conditioning procedure caused by Al deposition due to its high standard electrode potential (i.e., -1.66 V). In addition, YCl_3 can eliminate trace of water in the electrolyte due to its high reactivity with water. As a result, the $\text{MgCl}_2\text{-YCl}_3$ electrolyte displayed a low overpotential (i.e., 0.11 V), high Coulombic efficiency ($\approx 98.7\%$) and high anodic stability (i.e., 3 V vs Mg/Mg^{2+}) during Mg plating and stripping. Combined with a designed polysulfide cathode, the Mg–S battery using this $\text{MgCl}_2\text{-YCl}_3$ electrolyte delivered a discharge capacity over 1000 mAh g^{-1} for more than 50 cycles.^[17b] These excellent results indicate that all-inorganic electrolytes have strong application potentials for Mg–S batteries.

5.2.3. Simple Salt-Based Electrolytes

Simple Mg salts as electrolytes have advantages including ease of synthesis, better sulfur cathode compatibility, high ionic conductivity, and high anodic stability. Unfortunately, most of these simple salt electrolytes are incompatible with Mg anodes since they are reduced on a Mg surface, forming a Mg ion-insulating or poorly conductive layer, which inhibits migration of Mg ions to the Mg electrode surface. For example, $\text{Mg}(\text{PF}_6)_2$, and $\text{Mg}(\text{ClO}_4)_2$ tend to form an impermeable passivation layer on the surface of Mg anode, making successful Mg deposition not achievable.^[36a,61] Mg plating and stripping can be accomplished under a large overpotential in $\text{Mg}(\text{TFSI})_2$ (i.e., $\text{Mg}[\text{N}(\text{SO}_2\text{CF}_3)_2]_2$) and $\text{Mg}(\text{CF}_3\text{SO}_3)_2$ salts due to the formation of a low Mg ion conductive layer on Mg anode.^[62] Nevertheless, $\text{Mg}(\text{TFSI})_2$ without incorporation of any additional anions usually has low Coulombic efficiency, a large overpotential and low Mg plating/stripping kinetics due to formation of a passive surface upon the inevitable presence of traces of moisture.^[24b,26,28b,55,57a,63] To this end, MgCl_2 or $\text{Mg}(\text{BH}_4)_2$ are often added to help obtain stable and reversible Mg plating/stripping using $\text{Mg}(\text{TFSI})_2$ salt.^[64] The addition of Cl^- impedes passivation of Mg anode through formation of adsorbed Cl^- and/or MgCl_2 on the Mg anode surface and facilitates reversible Mg deposition and stripping by forming complex $[\text{Mg}_2(\mu\text{-Cl})_2]^{2+}$, as intermediate, to stabilize Mg^{2+} cations.^[26,42a,65]

To improve the electrochemical performance of simple Mg salts, many strategies have been developed. In 2014, Ha et al. developed a electrolyte based on glymes with $\text{Mg}(\text{TFSI})_2$ for rechargeable Mg and Mg–S batteries. The electrolyte exhibited an extremely high anodic stability exceeding 4.0 V with Al current collectors. When tested in a Mg–S battery using CMK-3/S as cathode, the $\text{Mg}(\text{TFSI})_2$ based electrolyte displayed a discharge capacity of 500 mAh g^{-1} and a potential plateau of 0.2 V.^[61] One of the advantages of simple Mg salt electrolyte is that it can adopt the well-established strategies of Li–S systems to address similar issues in Mg–S batteries. For example, Gao et al. employed the concentrated electrolyte concept to overcome the dissolution and diffusion issues of Mg polysulfide (see details in Figure 8).^[24b] By increasing the $\text{Mg}(\text{TFSI})_2$ concentration in $\text{Mg}(\text{TFSI})_2\text{-MgCl}_2\text{-DME}$ electrolyte from 0.25 M to 1 M, the Coulombic efficiency and cyclability were much improved through suppressing dissolution of polysulfides. The resulting Mg–S battery cycled more than 100 times with an initial capacity of about 800 mAh g^{-1} .^[24b] Hebié et al. proposed

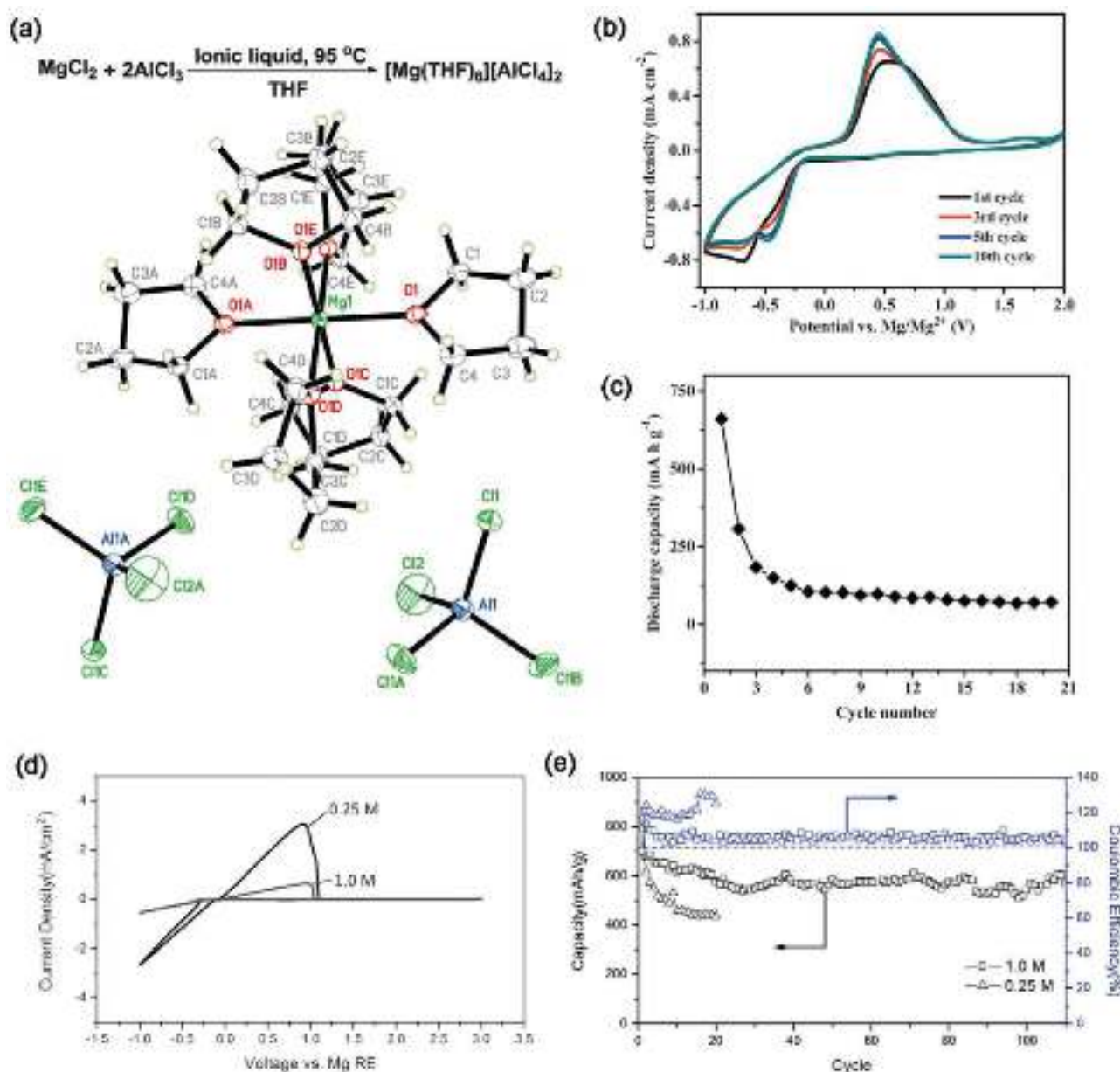


Figure 8. Characterization and performance of a-c) a MACC electrolyte and d,e) a simple salt electrolyte. a) Formation mechanism and X-ray crystal structure of the MACC salt $[Mg(THF)_6][AlCl_4]_2$. b) Cyclic voltammogram of electrolyte $[Mg(THF)_6][AlCl_4]_2$ in PYR14TFSI/THF. c) Cyclability of the Mg-S battery in $[Mg(THF)_6][AlCl_4]_2$ electrolyte. Reproduced with permission.^[60] Copyright 2016, Wiley-VCH. d) Mg deposition/stripping and anodic stability on Pt in $MgTFSI_2/MgCl_2/DME$ electrolyte. Reproduced with permission.^[24b] Copyright 2017, Wiley-VCH.

using a π -bond-rich molecule, anthracene as Mg coordinating agent to improve Mg plating/stripping.^[57a] The $Mg(TFSI)_2$ -anthracene electrolyte exhibited reversible Mg plating/stripping with a high anodic stability greater than 3 V. By adding $MgCl_2$, some nonuniform reactions on Mg/electrolyte interfaces were improved, enabling enhanced cyclability of Mg/Mo $_6$ S $_8$ Chevrel phase cells.^[57a] Application of simple Mg salts are mainly limited by the overpotential caused by the passivation layer (poorly ion conductive) formed on the surface of Mg metal. Adjusting the composition of this passivation layer could transform it to a Mg^{2+} ion-conductive one, therefore reducing the overpotential.

Li et al. proposed a strategy to reduce the overpotential by forming an Mg^{2+} ion conductive surface layer by adding a small concentration of iodine into $Mg(TFSI)_2$ -DME electrolyte.^[66] The resulting $Mg(TFSI)_2$ -DME-I $_2$ electrolyte facilitated formation of an insoluble MgI_2 layer that acted as the SEI on Mg anodes. By adopting this strategy, the obtained Mg-S batteries showing decreased voltage hysteresis owing to the reduced Mg deposition/stripping overpotentials.^[66]

Another commonly used simple salt is Mg trifluoromethanesulfonate (i.e., $Mg(CF_3SO_3)_2$).^[67] $Mg(CF_3SO_3)_2$ salt has similar advantages and issues as $Mg(TFSI)_2$ salt. A coordinating ligand

Table 3. Physical properties of typical solvents for magnesium battery electrolytes.

Solvent	Donor number [kcal mol ⁻¹]	Boiling point [°C]	Viscosity [mPa s]	Conductivity [mS cm ⁻¹]
THF	20	66	0.456	N/A
Glyme	24	85	0.455	N/A
Diglyme	19.5	162	1.089	N/A
Triglyme	N/A	216	1.6	N/A
Tetraglyme	16.6	275	4.01	N/A
AN	14.1	81	0.369	N/A
BMIM-Tf2N	low	16 (melting point)	45 ^[80]	3.9 ^[81]
PP13-Tf2N	low	8 (melting point)	129 ^[82]	1.5 ^[83]
DEME-BF ₄	low	45 (melting point)	1200 ^[84]	4.8 ^[84]

is also needed to stabilize Mg²⁺ ion in Mg(CF₃SO₃)₂ electrolyte. Yang et al. reported a Mg electrolyte through reaction between Mg(CF₃SO₃)₂ and AlCl₃ in THF. MgCl₂ was added to accelerate this reaction and improve the Mg/electrolyte interface properties. The π -containing molecule anthracene was used as a stabilizing agent for Mg ions. The Mg–S battery using this electrolyte showed high Coulombic efficiency and low overpotential and did not need conditioning. However, the initial capacity was low (i.e., 129.5 mAh g⁻¹) and it decayed quickly (i.e., 40 mAh g⁻¹) after 50 cycles.^[67a] Huang et al. improved the Mg(CF₃SO₃)₂-MgCl₂-AlCl₃ electrolyte by using DME as solvent. Their electrolyte displayed a high reversibility (i.e., Coulombic efficiency beyond 99.1%), low overpotential (i.e., 250 mV) and high anodic stability (i.e., 3.5 V) after conditioning. The discharge capacity of Mg–S battery was 866 mAh g⁻¹ at the first cycle and 450 mAh g⁻¹ at the 100th cycle.^[67b] To foster broader application of simple Mg salt electrolytes, several challenges are required to be overcome, including lowering the overpotential, improving the Coulombic efficiency, and raising oxidative stability.

5.3. Solvents Selection for Mg Electrolytes

As an important part of the electrolyte, the nature of the solvent greatly affects the electrochemical performance and safety of the electrolyte. The properties that an ideal solvent should have include high dielectric constant, high polarity, suitable viscosity, wide freezing/boiling temperature range, and wide electrochemical window.^[68] But so many properties are difficult to satisfy with one solvent, because some properties are mutually exclusive. For example, a single solvent cannot have a high dielectric constant and low viscosity at the same time. Therefore, a mixture of solvents and additives is often used for developing battery electrolyte. As an example, a binary mixture, with one solvent selected for solvation and the other for viscosity, is a commonly used solvent. Although carbonate-based solvents have proved to be more stable to anodization than ether solvents, they are not compatible with Mg anodes because they form a blocking film at the interface between Mg anodes and carbonate solvents.^[69] Therefore, the commonly used solvents for Mg-based batteries include ether solvents (e.g., THF, DME, diglyme, triglyme, tetraglyme (TEGDME) etc.), ionic liquid, and some polar solvents (e.g., acetonitrile (AN)).

Table 3 lists the physical properties of common solvents for magnesium batteries. THF is a popular solvent, and many Mg electrolytes have been developed using it. Some of them can only be obtained in THF (e.g., [Mg₂(μ -Cl)₃·6THF][HMDSAAlCl₃]). However, it is flammable and such volatile characteristics cause safety hazards. Glymes are widely used in Li–S batteries due to their relatively high boiling points, ideal viscosity, limited solubility of sulfur, good chemical stability against reactive metals and compatibility with sulfide/polysulfide nucleophilic anions.^[58,70] Ha et al. used a binary mixture of glyme/diglyme to develop a simple salt Mg(TFSI)₂ Mg electrolyte. Glyme and diglyme exhibit low overpotentials in Mg plating and stripping while triglyme and tetraglyme solvents with long ether chains show extremely large overpotentials. Addition of glyme into diglyme can increase its ionic conductivity. Therefore, a glyme/diglyme (1/1, v/v) mixture was selected by Ha's group as the electrolyte solvent.^[61] Bevilacqua et al. studied the effects of various solvents including THF, DME, DOL, tetraglyme on Mg electrodeposition, S₈ reduction, and MgS oxidation in Mg–S batteries in MACC electrolyte. Reversible Mg plating and stripping have been demonstrated in various solvent systems including DME, DME/DOL, tetraglyme/DOL, and tetraglyme/THF. Bevilacqua et al. also found that the peak reduction potential and cathodic current are dependent on the electrolyte solvents, suggesting a solvent-mediated reduction pathway of S₈ cathode.^[71] Through calculation using first principle theory and molecule dynamics, Rajput et al. reported that higher order glymes were beneficial for the dissolution of Mg salts, but harmful for the ion dynamics in solution. Attaining solvation of Mg salts is critical as they are prone to form contact ion pair and aggregates in most organic solvents. The authors also claim that the dielectric constant of solvents is not the determinant for the solvation of Mg salts. More complex, the molecular-scale feature of the solvents, including the molecular size, oxygen/nitrogen density and chelation, showed great effects on the dissolution of Mg salts.^[55]

Ionic liquids, known as molten salts with a melting point below 100 °C, are employed as another type of solvent for battery electrolytes. Ionic liquids are comprised completely of ions and have a variety of superior physicochemical properties, such as low vapor pressure, nonflammability, high chemical and thermal stability, high ionic conductivity, and a wide electrochemical window.^[72] Therefore, ionic liquids have been applied as a cosolvent in LIBs, Li–S battery and novel chloride ion

batteries.^[73] In metal–sulfur battery, ionic liquids can help inhibit polysulfide dissolution by adjusting the viscosity of the electrolyte. Zhao-Karger et al. used a binary solvent mixture of glyme and ionic liquid to develop an amide-based electrolyte (active product is $[\text{Mg}_2\text{Cl}_3][\text{HMDSA}(\text{AlCl}_3)]$).^[24c] The addition of an ionic liquid improves performance of Mg–S battery by 1) retarding the diffusion of the polysulfide to the anode side through increasing the electrolyte viscosity and 2) lowering the solubility of polysulfide due to the weakly coordinating TFSI^- anion from the ionic liquid.^[24c] However, using ionic liquid alone as a simple Mg salt electrolyte solvent does not seem to work. Vardar et al. studied the Mg plating process of several simple Mg salts (i.e., $\text{Mg}(\text{Tf}_2\text{N})_2$, $\text{Mg}(\text{TfO})_2$, and $\text{Mg}(\text{BH}_4)_2$) dissolved in several ionic liquids (i.e., BMMIM- Tf_2N , PP13- Tf_2N and DEME- BF_4). However, none of these salt/ionic liquid combinations facilitated reversible Mg plating. Their results show that simple Mg salts are not satisfactory when used in ionic liquid electrolyte for Mg–S batteries.^[74] Such varying reports indicate that further investigations are still needed on Mg electrolyte solvents. The development of efficient electrolytes for Mg–S batteries needs to overcome a key challenge by developing a new solvent with low solubility of polysulfides and sulfur.

5.4. Corrosivity of Mg Electrolytes

When electrolyte corrosion occurs, the metallic atoms in batteries are oxidized to soluble metal cations and leave holes, pits, or a thinning of the component. Corrosion can be observed through measuring the oxidative current flow especially under a low potential. The electrochemical corrosion is categorized as “pitting corrosion” and “uninhibited corrosion” according to whether the corrosion area can be healed by formation of passivation films.^[12] Corrosion should be avoided as it jeopardizes the performance, safety, and lifetime of a battery. For example, oxidized metal cations may also participate in plating processes and forming dendrites, causing internal short-circuiting. Unfortunately, many organohaloaluminate electrolytes are corrosive to non-noble metal current collectors (Al, Cu, etc.). For example, Al, Cu stainless-steel, and Ni exhibit very low anodic stability of 1.2, 1.9, 2.0, and 2.1 V (vs Mg RE) in APC electrolyte due to corrosion.^[75] In 2012, Guo et al. reported that a Mg electrolyte with a chlorinated cation, $\text{Mg}_2(\mu\text{-Cl})_3 \cdot 6\text{THF}$ and a nonchlorinated anion showed high oxidation stability above 3 V on Al and Ni electrodes but low oxidation stability of 2.2 V on stainless steel electrodes, indicating the corrosive nature of the electrolyte with stainless steel.^[76] In 2013, Muldoon et al. showed experimentally that Mg electrolyte that do not contain chlorine in both salt ions (e.g., organomagnesium borates) is noncorrosive.^[36a] These studies proved that corrosion comes from chlorine. Therefore, developing chloride-free Mg salt is an effective way to obtain noncorrosive Mg electrolyte.

To date, all-inorganic electrolyte with nonchlorinated cations, boron-based Mg electrolytes with nonchlorinated cations and simple Mg salt electrolytes have been investigated as less/noncorrosive electrolytes, as discussed above. Although most simple magnesium salts do not contain chlorine, it was often regarded as necessary to add MgCl_2 to make up for their performance deficiencies, such as low Coulombic efficiency, a large overpotential, and low Mg plating/stripping kinetic.

6. Perspectives

Although increasing efforts have been dedicated to rechargeable Mg–S batteries in recent years, Mg–S battery know-how is still in an infant stage. Most Mg–S batteries tests have been performed under mild conditions far from practical requirements (e.g., low sulfur contents $\approx 20\text{--}40\%$) in cathodes and flooded electrolyte amounts (electrolyte/sulfur ratio ≥ 20). Even so, the battery performance is still unsatisfactory in terms of cyclability (mostly < 200 cycles), charge-discharge overpotential (> 1 V), Coulombic efficiency and rate capability. The reason for this current state of play is that the main challenges in Mg–S batteries have not yet been resolved. In this section, we list the main remaining challenges and possible corresponding resolutions, and call for attention from the research and innovation community to focus on them in future research for practical and advanced Mg–S batteries.

6.1. Mg Polysulfide Solubility Enhancement

In contrast to Li–S batteries where the main challenge is the shuttle effect of Li polysulfides, the low solubility of long chain Mg polysulfides is the main issue in Mg–S batteries, because this is the main culprit of performance degradation. The low solubility of long chain Mg polysulfides renders most sulfur immobilized in a solid state, especially at high sulfur content and/or in lean electrolytes, which results in low utilization of sulfur and hence a decrease in discharge capacity.^[13] In addition, the small amount of dissolved long chain Mg polysulfides, as key electron intermediates for liquid–solid reaction with fast kinetics, will be depleted rapidly, causing the electrochemical reaction to enter a slow solid–solid reaction, whereby Mg^{2+} ions diffuse sluggishly from the electrolyte into the solid-state MgS_x and S. This leads to a rapid drop in discharge voltage, low Coulombic efficiency and poor rate capability. Therefore, rather than limiting the solubility of Li polysulfides in Li–S batteries to inhibit the shuttle effect, future research should increase the solubility of Mg polysulfides to enhance the battery performance and promote its practical application. To do so, more work should be devoted to developing new solvent formulations and to design functional additives. The current Mg–S electrolyte solvent formulation is designed to enhance the solubility and mobility of the Mg salt, and it has not been considered to enhance the solubility of Mg polysulfides. In order to enhance these solubilities, a single solvent may not be adequate, and a mixture of two or more solvents is required to achieve multifunctionality. More work is needed on this in the future. In addition, designing additives that have a strong interaction with Mg polysulfides may be another effective way to enhance the dissolution of Mg polysulfides. The design principles of these functional additives should include: 1) enhancing the dissolution of magnesium polysulfide; 2) not reducing the performance of electrolyte; 3) inert to magnesium metal electrode. Highly soluble polysulfides, however, may exacerbate ineffective shuttle effect, which should be inhibited through design of other battery components (e.g., CNF-coated separators and protective layers on anodes).^[24a,62] In addition, some techniques to increasing the sulfur utilization in Li–S batteries are still

applicable to Mg-S batteries, including improving the contact between elemental sulfur and carbon matrix, increasing electronic conductivity of carbon matrix or developing more conducting transition metal sulfides.^[42b,77]

6.2. Anode Solid Layer Control

In a Mg-S battery, the high overpotential of the battery during cycling is mainly derived from the Mg anode due to its impedance being much higher than that of a sulfur cathode.^[14a] The high impedance is due to a solid layer formed on the Mg anode via electrolyte decomposition or reaction with traces of water and oxygen. Therefore, developing a suitable electrolyte that inhibits the formation of blocking layers on Mg anodes is required to address the overpotential issue. Although it is reported that adding MgCl_2 or AlCl_3 to electrolyte can improve Mg deposition (i.e., decreasing the impedance of Mg anode) by forming adsorbed Cl^- on the surface of the Mg anode, added Cl will likely cause corrosion of some battery components, such as current collectors.^[17a,26,42a,65] The preferential decomposition of ligands coordinated to Mg^{2+} ions is one of the main reasons for the formation of a blocking layer on Mg anodes. Boron-centered anion-based magnesium (BCM) is suggested as a promising candidate to address all the above issues. First, the large weakly-bonded boron-centered anion that readily dissociates from Mg^{2+} can avoid reduction at the anode surface, therefore inhibiting the formation of a blocking layer. Second, low-chlorine-residue boron-centered anions prevent corrosion issues. Third, boron-centered anions provide a platform to develop electrolytes with high anodic stability and reversibility via designing functional groups grafted on the central boron atom. In addition, BCM salt is air and water insensitive, which is beneficial for commercial applications.

6.3. Kinetics Improvement

The sluggish kinetics of Mg-S electrochemical reactions is probably the biggest obstacle to the development of advanced Mg-S batteries. The sluggish kinetics is due to the solid-solid reaction of MgS_2 to MgS , leading to a sharp potential drop from 1.5 to 0.5 V and early termination of discharge.^[13] To improve the reaction kinetics, future research is suggested to focus on developing the approaches that can increase the activity and/or solubility of both MgS_2 and MgS . For example, using a Lewis acid mediator to activate MgS , or adding TiS_2 as a catalyst to activate short-chain Mg polysulfides has been proven to be an effective method to improve the reaction kinetics, thereby achieving better cyclability.^[14b] Besides, many catalysts developed to improve reaction kinetics in Li-S, Na-S, and K-S batteries may be transferred to Mg-S batteries and their catalytic effects in Mg-S batteries are waiting to be discovered. In addition, developing functional electrolyte is a feasible way to improve kinetics by increased solubility of short chain magnesium polysulfides.

In summary, addressing current challenges facing Mg-S batteries will mainly rely on the design and development of electrolyte. Despite the research being at an early stage of

achievements, we believe that, with great efforts devoted to the above-mentioned research directions, the challenges associated with materials and system in Mg-S batteries can be successfully addressed in the near future, which will promote the transition of Mg-S batteries into practical application.

Acknowledgements

Y.L. would like to acknowledge “Qilu Young Scholar” Program of Shandong University (Grant No. 11500082063143) and a Discovery Early Career Researcher Award Fellowship (No. DE190100082). X.Z. would like to acknowledge “Startup Project for High-level Talents of Shandong University of Technology” (Grant No. 4041-420119). Z.G. would like to acknowledge the Australian Research Council for its support through a Discovery project (No. DP200101862) and a Linkage project (No. LP160101629).

Conflict of Interest

The authors declare no conflict of interest.

Keywords

magnesium-sulfur batteries, magnesium-sulfur electrochemistry, Mg electrolytes, Mg polysulfides, Mg solid layer control

Received: December 30, 2020

Revised: March 5, 2021

Published online: April 14, 2021

- [1] a) J. W. Choi, D. Aurbach, *Nat. Rev. Mater.* **2016**, 1, 16013; b) R. E. Doe, R. Han, J. Hwang, A. J. Gmitter, I. Shterenberg, H. D. Yoo, N. Pour, D. Aurbach, *Chem. Commun.* **2014**, 50, 243; c) B. Dunn, H. Kamath, J. M. Tarascon, *Science* **2011**, 334, 928; d) Y. Liu, Z. Tai, T. Zhou, V. Sencadas, J. Zhang, L. Zhang, K. Konstantinov, Z. Guo, H. K. Liu, *Adv. Mater.* **2017**, 29, 1703028.
- [2] a) J. B. Goodenough, K. S. Park, *J. Am. Chem. Soc.* **2013**, 135, 1167; b) J. Liu, Z. Bao, Y. Cui, E. J. Dufek, J. B. Goodenough, P. Khalifah, Q. Li, B. Y. Liaw, P. Liu, A. Manthiram, *Nat. Energy* **2019**, 4, 180; c) G. Liang, Z. Wu, C. Didier, W. Zhang, J. Cuan, B. Li, K. Y. Ko, P. Y. Hung, C. Z. Lu, Y. Chen, G. Leniec, S. M. Kaczmarek, B. Johannessen, L. Thomsen, V. K. Peterson, W. K. Pang, Z. Guo, *Angew. Chem., Int. Ed.* **2020**, 59, 10594.
- [3] a) S. Hu, Y. Li, Y. Chen, J. Peng, T. Zhou, W. K. Pang, C. Didier, V. K. Peterson, H. Wang, Q. Li, Z. Guo, *Adv. Energy Mater.* **2019**, 9, 1901795; b) S. Kalluri, M. Yoon, M. Jo, S. Park, S. Myeong, J. Kim, S. X. Dou, Z. Guo, J. Cho, *Adv. Energy Mater.* **2017**, 7, 1601507; c) Y. Zheng, T. Zhou, X. Zhao, W. K. Pang, H. Gao, S. Li, Z. Zhou, H. Liu, Z. Guo, *Adv. Mater.* **2017**, 29, 1700396.
- [4] a) H. Wang, W. Zhang, J. Xu, Z. Guo, *Adv. Funct. Mater.* **2018**, 28, 1707520; b) Z. Li, H. B. Wu, X. W. Lou, *Energy Environ. Sci.* **2016**, 9, 3061; c) Z. Li, B. Y. Guan, J. Zhang, X. W. Lou, *Joule* **2017**, 1, 576.
- [5] a) M. S. Whittingham, *Chem. Rev.* **2004**, 104, 4271; b) G. Li, S. Wang, Y. Zhang, M. Li, Z. Chen, J. Lu, *Adv. Mater.* **2018**, 30, 1705590; c) X. Zhao, Y. Lu, Z. Qian, R. Wang, Z. Guo, *EcoMat* **2020**, 2, e12038.
- [6] X. Ji, K. T. Lee, L. F. Nazar, *Nat. Mater.* **2009**, 8, 500.
- [7] a) X. Hong, J. Mei, L. Wen, Y. Tong, A. J. Vasiloff, L. Wang, J. Liang, Z. Sun, S. X. Dou, *Adv. Mater.* **2019**, 31, 1802822; b) Y. Liang, H. Dong, D. Aurbach, Y. Yao, *Nat. Energy* **2020**, 5, 646.

- [8] a) Z. Wang, Y. Wang, Z. Zhang, X. Chen, W. Lie, Y. B. He, Z. Zhou, G. Xia, Z. Guo, *Adv. Funct. Mater.* **2020**, *30*, 2002414; b) J. Wang, S. Yi, J. Liu, S. Sun, Y. Liu, D. Yang, K. Xi, G. Gao, A. Abdelkader, W. Yan, *ACS Nano* **2020**, *14*, 9819; c) J. Wu, J. Liu, Z. Lu, K. Lin, Y. Q. Lyu, B. Li, F. Ciucci, J. K. Kim, *Energy Storage Mater.* **2019**, *23*, 8.
- [9] a) P. Wang, M. Buchmeiser, *Adv. Funct. Mater.* **2019**, *29*, 1905248; b) Z. Zhang, S. Dong, Z. Cui, A. Du, G. Li, G. Cui, *Small Methods* **2018**, *2*, 1800020; c) Z. Guo, S. Zhao, T. Li, D. Su, S. Guo, G. Wang, *Adv. Energy Mater.* **2020**, *10*, 1903591; d) X. Cheng, Z. Zhang, Q. Kong, Q. Zhang, T. Wang, S. Dong, L. Gu, X. Wang, J. Ma, P. Han, *Angew. Chem., Int. Ed.* **2020**, *59*, 11477; e) Z. Zhang, B. Chen, H. Xu, Z. Cui, S. Dong, A. Du, J. Ma, Q. Wang, X. Zhou, G. Cui, *Adv. Funct. Mater.* **2018**, *28*, 1701718.
- [10] Z. Zhao-Karger, M. Fichtner, *MRS Commun.* **2017**, *7*, 770.
- [11] a) L. Kong, C. Yan, J. Q. Huang, M. Q. Zhao, M. M. Titirici, R. Xiang, Q. Zhang, *Energy Environ. Sci.* **2018**, *1*, 100; b) M. Mao, T. Gao, S. Hou, C. Wang, *Chem. Soc. Rev.* **2018**, *47*, 8804.
- [12] J. Muldoon, C. B. Bucur, T. Gregory, *Angew. Chem., Int. Ed.* **2017**, *56*, 12064.
- [13] T. Gao, X. Ji, S. Hou, X. Fan, X. Li, C. Yang, F. Han, F. Wang, J. Jiang, K. Xu, *Adv. Mater.* **2018**, *30*, 1704313.
- [14] a) B. P. Vinayan, H. Euchner, Z. Zhao-Karger, M. A. Cambaz, Z. Li, T. Diemant, R. J. Behm, A. Gross, M. Fichtner, *J. Mater. Chem. A* **2019**, *7*, 25490; b) Y. Xu, Y. Ye, S. Zhao, J. Feng, J. Li, H. Chen, A. Yang, F. Shi, L. Jia, Y. Wu, *Nano Lett.* **2019**, *19*, 2928.
- [15] Y. Nakayama, Y. Kudo, H. Oki, K. Yamamoto, Y. Kitajima, K. Noda, *J. Electrochem. Soc.* **2008**, *155*, A754.
- [16] B. Vinayan, Z. Zhao-Karger, T. Diemant, V. S. K. Chakravadhanula, N. I. Schwarzbürger, M. A. Cambaz, R. J. Behm, C. Kübel, M. Fichtner, *Nanoscale* **2016**, *8*, 3296.
- [17] a) H. S. Kim, T. S. Arthur, G. D. Allred, J. Zajicek, J. G. Newman, A. E. Rodnyansky, A. G. Oliver, W. C. Boggess, J. Muldoon, *Nat. Commun.* **2011**, *2*, 1; b) Y. Xu, G. Zhou, S. Zhao, W. Li, F. Shi, J. Li, J. Feng, Y. Zhao, Y. Wu, J. Guo, *Adv. Sci.* **2019**, *6*, 1800981; c) H. Du, Z. Zhang, J. He, Z. Cui, J. Chai, J. Ma, Z. Yang, C. Huang, G. Cui, *Small* **2017**, *13*, 1702277.
- [18] T. A. Pascal, K. H. Wujcik, J. Velasco-Velez, C. Wu, A. A. Teran, M. Kapilashrami, J. Cabana, J. Guo, M. Salmeron, N. Balsara, *J. Phys. Chem. Lett.* **2014**, *5*, 1547.
- [19] W. Wang, H. Yuan, Y. NuLi, J. Zhou, J. Yang, J. Wang, *J. Phys. Chem. C* **2018**, *122*, 26764.
- [20] L. Zeng, N. Wang, J. Yang, J. Wang, Y. Nuli, *J. Electrochem. Soc.* **2017**, *164*, A2504.
- [21] X. Zhou, J. Tian, J. Hu, C. Li, *Adv. Mater.* **2018**, *30*, 1704166.
- [22] J. Sun, C. Deng, Y. Bi, K. H. Wu, S. Zhu, Z. Xie, C. Li, R. Amal, J. Luo, T. Liu, *ACS Appl. Energy Mater.* **2020**, *3*, 2516.
- [23] M. Frey, R. K. Zenn, S. Warneke, K. Müller, A. Hintennach, R. E. Dinnebier, M. R. Buchmeiser, *ACS Energy Lett.* **2017**, *2*, 595.
- [24] a) X. Yu, A. Manthiram, *ACS Energy Lett.* **2016**, *1*, 431; b) T. Gao, S. Hou, F. Wang, Z. Ma, X. Li, K. Xu, C. Wang, *Angew. Chem., Int. Ed.* **2017**, *129*, 13711; c) Z. Zhao-Karger, X. Zhao, D. Wang, T. Diemant, R. J. Behm, M. Fichtner, *Adv. Energy Mater.* **2015**, *5*, 1401155.
- [25] D. Aurbach, Y. Gofer, Z. Lu, A. Schechter, O. Chusid, H. Gizbar, Y. Cohen, V. Ashkenazi, M. Moshkovich, R. Turgeman, *J. Power Sources* **2001**, *97*, 28.
- [26] J. G. Connell, B. Genorio, P. P. Lopes, D. Strmcnik, V. R. Stamenkovic, N. M. Markovic, *Chem. Mater.* **2016**, *28*, 8268.
- [27] T. Gao, S. Hou, K. Huynh, F. Wang, N. Eidson, X. Fan, F. Han, C. Luo, M. Mao, X. Li, *ACS Appl. Mater. Interfaces* **2018**, *10*, 14767.
- [28] a) I. Shterenberg, M. Salama, H. D. Yoo, Y. Gofer, J. B. Park, Y. K. Sun, D. Aurbach, *J. Electrochem. Soc.* **2015**, *162*, A7118; b) H. D. Yoo, S.-D. Han, I. L. Bolotin, G. M. Nolis, R. D. Bayliss, A. K. Burrell, J. T. Vaughey, J. Cabana, *Langmuir* **2017**, *33*, 9398; c) T. S. Arthur, P. A. Glans, N. Singh, O. Tutusaus, K. Nie, Y. S. Liu, F. Mizuno, J. Guo, D. H. Alsem, N. Salmon, *Chem. Mater.* **2017**, *29*, 7183.
- [29] Z. Lu, A. Schechter, M. Moshkovich, D. Aurbach, *J. Electroanal. Chem.* **1999**, *466*, 203.
- [30] X. C. Hu, Y. Shi, S. Y. Lang, X. Zhang, L. Gu, Y. G. Guo, R. Wen, L. J. Wan, *Nano Energy* **2018**, *49*, 453.
- [31] a) A. Kitada, K. Nakamura, K. Fukami, K. Murase, *Electrochim. Acta* **2016**, *217*, 561; b) A. Kitada, Y. Kang, K. Matsumoto, K. Fukami, R. Hagiwara, K. Murase, *J. Electrochem. Soc.* **2015**, *162*, D389; c) Y. Shao, T. Liu, G. Li, M. Gu, Z. Nie, M. Engelhard, J. Xiao, D. Lv, C. Wang, J. G. Zhang, *Sci. Rep.* **2013**, *3*, 1.
- [32] F. Tuerxun, K. Yamamoto, M. Hattori, T. Mandai, K. Nakanishi, A. Choudhary, Y. Tateyama, K. Sodeyama, A. Nakao, T. Uchiyama, M. Matsui, K. Tsuruta, Y. Tamenori, K. Kanamura, Y. Uchimoto, *ACS Appl. Mater. Interfaces* **2020**, *12*, 25775.
- [33] a) N. Singh, T. S. Arthur, C. Ling, M. Matsui, F. Mizuno, *Chem. Commun.* **2013**, *49*, 149; b) T. S. Arthur, N. Singh, M. Matsui, *Electrochem. Commun.* **2012**, *16*, 103; c) F. Murgia, E. T. Weldekidan, L. Stievano, L. Monconduit, R. Berthelot, *Electrochem. Commun.* **2015**, *60*, 56; d) K. Periyapperuma, T. T. Tran, M. Purcell, M. Obrovac, *Electrochim. Acta* **2015**, *165*, 162.
- [34] a) D. T. Nguyen, S. W. Song, *J. Power Sources* **2017**, *368*, 11; b) Y. H. Tan, W. T. Yao, T. Zhang, T. Ma, L. L. Lu, F. Zhou, H. B. Yao, S. H. Yu, *ACS Nano* **2018**, *12*, 5856.
- [35] Z. Meng, D. Foix, N. Brun, R. Dedryvère, L. Stievano, M. Morcrette, R. Berthelot, *ACS Energy Lett.* **2019**, *4*, 2040.
- [36] a) J. Muldoon, C. B. Bucur, A. G. Oliver, J. Zajicek, G. D. Allred, W. C. Boggess, *Energy Environ. Sci.* **2013**, *6*, 482; b) D. Aurbach, Y. Gofer, A. Schechter, O. Chusid, H. Gizbar, Y. Cohen, M. Moshkovich, R. Turgeman, *J. Power Sources* **2001**, *97*, 269; c) J. Gnanaraj, V. Pol, A. Gedanken, D. Aurbach, *Electrochem. Commun.* **2003**, *5*, 940.
- [37] a) J. H. Connor, W. E. Reid Jr., G. B. Wood, *J. Electrochem. Soc.* **1957**, *104*, 38; b) C. Liebenow, *J. Appl. Electrochem.* **1997**, *27*, 221.
- [38] T. D. Gregory, R. J. Hoffman, R. C. Winterton, *J. Electrochem. Soc.* **1990**, *137*, 775.
- [39] D. Aurbach, Z. Lu, A. Schechter, Y. Gofer, H. Gizbar, R. Turgeman, Y. Cohen, M. Moshkovich, E. Levi, *Nature* **2000**, *407*, 724.
- [40] H. Gizbar, Y. Vestfrid, O. Chusid, Y. Gofer, H. E. Gottlieb, V. Marks, D. Aurbach, *Organometallics* **2004**, *23*, 3826.
- [41] a) D. Aurbach, H. Gizbar, A. Schechter, O. Chusid, H. E. Gottlieb, Y. Gofer, I. Goldberg, *J. Electrochem. Soc.* **2001**, *149*, A115; b) Y. Gofer, O. Chusid, H. Gizbar, Y. Vestfrid, H. E. Gottlieb, V. Marks, D. Aurbach, *Electrochem. Solid-State Lett.* **2006**, *9*, A257.
- [42] a) N. Pour, Y. Gofer, D. T. Major, D. Aurbach, *J. Am. Chem. Soc.* **2011**, *133*, 6270; b) D. Aurbach, G. S. Suresh, E. Levi, A. Mitelman, O. Mizrahi, O. Chusid, M. Brunelli, *Adv. Mater.* **2007**, *19*, 4260.
- [43] C. J. Barile, R. Spatney, K. R. Zavadil, A. A. Gewirth, *J. Phys. Chem. C* **2014**, *118*, 10694.
- [44] C. Liebenow, Z. Yang, P. Lobitz, *Electrochem. Commun.* **2000**, *2*, 641.
- [45] T. Gao, M. Noked, A. J. Pearce, E. Gillette, X. Fan, Y. Zhu, C. Luo, L. Suo, M. A. Schroeder, K. Xu, *J. Am. Chem. Soc.* **2015**, *137*, 12388.
- [46] Y. Xu, W. Li, G. Zhou, Z. Pan, Y. Zhang, *Energy Storage Mater.* **2018**, *14*, 253.
- [47] X. Zhao, Y. Yang, Y. NuLi, D. Li, Y. Wang, X. Xiang, *Chem. Comm.* **2019**, *55*, 6086.
- [48] Y. Yang, Y. Qiu, Y. NuLi, W. Wang, J. Yang, J. Wang, *J. Mater. Chem. A* **2019**, *7*, 18295.
- [49] F. Wang, Y. Guo, J. Yang, Y. Nuli, S. Hirano, *Chem. Comm.* **2012**, *48*, 10763.
- [50] C. Liao, B. Guo, D. E. Jiang, R. Custelcean, S. M. Mahurin, X. G. Sun, S. Dai, *J. Mater. Chem. A* **2014**, *2*, 581.
- [51] Z. Zhao-Karger, M. E. G. Bardaji, O. Fuhr, M. Fichtner, *J. Mater. Chem. A* **2017**, *5*, 10815.
- [52] a) O. Tutusaus, R. Mohtadi, T. S. Arthur, F. Mizuno, E. G. Nelson, Y. V. Sevryugina, *Angew. Chem., Int. Ed.* **2015**, *127*, 8011; b) P. Saha, M. K. Datta, O. I. Velikokhatnyi, A. Manivannan, D. Alman, P. N. Kumta, *Prog. Mater. Sci.* **2014**, *66*, 1.

- [53] Z. Zhang, Z. Cui, L. Qiao, J. Guan, H. Xu, X. Wang, P. Hu, H. Du, S. Li, X. Zhou, *Adv. Energy Mater.* **2017**, 7, 1602055.
- [54] A. Du, Z. Zhang, H. Qu, Z. Cui, L. Qiao, L. Wang, J. Chai, T. Lu, S. Dong, T. Dong, *Energy Environ. Sci.* **2017**, 10, 2616.
- [55] N. N. Rajput, X. Qu, N. Sa, A. K. Burrell, K. A. Persson, *J. Am. Chem. Soc.* **2015**, 137, 3411.
- [56] W. E. Geiger, F. Barrière, *Acc. Chem. Res.* **2010**, 43, 1030.
- [57] a) S. Hebié, F. Alloin, C. Iojoiu, R. Berthelot, J. C. Leprêtre, *ACS Appl. Mater. Interfaces* **2018**, 10, 5527; b) M. Salama, R. Attias, B. Hirsch, R. Yemini, Y. Gofer, M. Noked, D. Aurbach, *ACS Appl. Mater. Interfaces* **2018**, 10, 36910.
- [58] Z. Zhao-Karger, R. Liu, W. Dai, Z. Li, T. Diemant, B. Vinayan, C. Bonatto Minella, X. Yu, A. Manthiram, R. J. r. Behm, *ACS Energy Lett.* **2018**, 3, 2005.
- [59] a) S. S. Kim, S. C. Bevilacqua, K. A. See, *ACS Appl. Mater. Interfaces* **2019**, 12, 5226; b) K. A. See, Y. M. Liu, Y. Ha, C. J. Barile, A. A. Gewirth, *ACS Appl. Mater. Interfaces* **2017**, 9, 35729.
- [60] W. Li, S. Cheng, J. Wang, Y. Qiu, Z. Zheng, H. Lin, S. Nanda, Q. Ma, Y. Xu, F. Ye, *Angew. Chem., Int. Ed.* **2016**, 128, 6516.
- [61] S. Y. Ha, Y. W. Lee, S. W. Woo, B. Koo, J. S. Kim, J. Cho, K. T. Lee, N. S. Choi, *ACS Appl. Mater. Interfaces* **2014**, 6, 4063.
- [62] Z. Zhou, B. Chen, T. Fang, Y. Li, Z. Zhou, Q. Wang, J. Zhang, Y. Zhao, *Adv. Energy Mater.* **2020**, 10, 1902023.
- [63] A. Baskin, D. Prendergast, *J. Phys. Chem. C* **2016**, 120, 3583.
- [64] a) N. Sa, B. Pan, A. Saha-Shah, A. A. Hubaud, J. T. Vaughey, L. A. Baker, C. Liao, A. K. Burrell, *ACS Appl. Mater. Interfaces* **2016**, 8, 16002; b) S. Hebié, H. P. K. Ngo, J. C. Leprêtre, C. Iojoiu, L. Cointeaux, R. Berthelot, F. Alloin, *ACS Appl. Mater. Interfaces* **2017**, 9, 28377.
- [65] a) Y. Vestfried, O. Chusid, Y. Goffer, P. Aped, D. Aurbach, *Organometallics* **2007**, 26, 3130; b) O. Mizrahi, N. Amir, E. Pollak, O. Chusid, V. Marks, H. Gottlieb, L. Larush, E. Zinigrad, D. Aurbach, *J. Electrochem. Soc.* **2007**, 155, A103; c) K. A. See, K. W. Chapman, L. Zhu, K. M. Wiaderek, O. J. Borkiewicz, C. J. Barile, P. J. Chupas, A. A. Gewirth, *J. Am. Chem. Soc.* **2016**, 138, 328.
- [66] X. Li, T. Gao, F. Han, Z. Ma, X. Fan, S. Hou, N. Eidson, W. Li, C. Wang, *Adv. Energy Mater.* **2018**, 8, 1701728.
- [67] a) Y. Yang, W. Wang, Y. Nuli, J. Yang, J. Wang, *ACS Appl. Mater. Interfaces* **2019**, 11, 9062; b) D. Huang, S. Tan, M. Li, D. Wang, C. Han, Q. An, L. Mai, *ACS Appl. Mater. Interfaces* **2020**, 12, 17474.
- [68] D. Aurbach, I. Weissman, *Nonaqueous electrochemistry: an overview*, Marcel Dekker, New York **1999**.
- [69] K. Xu, *Chem. Rev.* **2004**, 104, 4303.
- [70] a) C. Barchasz, J. C. Leprêtre, S. Patoux, F. Alloin, *J. Electrochem. Soc.* **2013**, 160, A430; b) C. Barchasz, J. C. Leprêtre, S. Patoux, F. Alloin, *Electrochim. Acta* **2013**, 89, 737; c) N. Tachikawa, K. Yamauchi, E. Takashima, J. W. Park, K. Dokko, M. Watanabe, *Chem. Commun.* **2011**, 47, 8157; d) Y. Zhang, S. Liu, G. Li, G. Li, X. Gao, *J. Mater. Chem. A* **2014**, 2, 4652.
- [71] S. Bevilacqua, K. H. Pham, K. A. See, *Inorg. Chem.* **2019**, 58, 10472.
- [72] a) K. Fujita, N. Nakamura, K. Igarashi, M. Samejima, H. Ohno, *Green Chem.* **2009**, 11, 351; b) J. S. Wilkes, M. J. Zaworotko, *J. Chem. Soc. Chem. Commun.* **1992**, 965.
- [73] a) M. Galiński, A. Lewandowski, I. Stępnik, *Electrochim. Acta* **2006**, 51, 5567; b) L. Wang, H. R. Byon, *J. Power Sources* **2013**, 236, 207; c) X. Zhao, Z. Zhao-Karger, D. Wang, M. Fichtner, *Angew. Chem., Int. Ed.* **2013**, 125, 13866; d) X. Zhao, S. Ren, M. Bruns, M. Fichtner, *J. Power Sources* **2014**, 245, 706.
- [74] G. Vardar, A. E. Sleightholme, J. Naruse, H. Hiramatsu, D. J. Siegel, C. W. Monroe, *ACS Appl. Mater. Interfaces* **2014**, 6, 18033.
- [75] J. Muldoon, C. B. Bucur, A. G. Oliver, T. Sugimoto, M. Matsui, H. S. Kim, G. D. Allred, J. Zajicek, Y. Kotani, *Energy Environ. Sci.* **2012**, 5, 5941.
- [76] Y. S. Guo, F. Zhang, J. Yang, F. F. Wang, Y. NuLi, S.-i. Hirano, *Energy Environ. Sci.* **2012**, 5, 9100.
- [77] X. Sun, P. Bonnick, V. Duffort, M. Liu, Z. Rong, K. A. Persson, G. Ceder, L. F. Nazar, *Energy Environ. Sci.* **2016**, 9, 2273.
- [78] D. Muthuraj, A. Ghosh, A. Kumar, S. Mitra, *ChemElectroChem* **2019**, 6, 684.
- [79] K. Itaoka, I. T. Kim, K. Yamabuki, N. Yoshimoto, H. Tsutsumi, *J. Power Sources* **2015**, 297, 323.
- [80] Z. Zhang, X. Gao, L. Yang, *Chin. Sci. Bull.* **2005**, 50.
- [81] P. Bonhôte, A.-P. Dias, N. Papageorgiou, K. Kalyanasundaram, M. Grätzel, *Inorg. Chem.* **1996**, 35, 1168.
- [82] N. Tachikawa, Y. Katayama, T. Miura, *ECS Trans.* **2009**, 16, 589.
- [83] H. Sakaebe, H. Matsumoto, *Electrochem. Commun.* **2003**, 5, 594.
- [84] T. Sato, G. Masuda, K. Takagi, *Electrochim. Acta* **2004**, 49, 3603.



Yan Lu is currently a professor at Shandong University. She obtained her Ph.D. degree from Shanghai Institute of Ceramics, Chinese Academy of Sciences in 2014, under the supervision of Prof. Zhaoyin Wen. She was a postdoctoral research fellow at Dr. Eileen Fong's group (2014–2016), Prof. Xiongwen (David) Lou's group (2016–2018), and Prof. Rong Xu's group (2018) at Nanyang Technological University, Singapore. She then got an ARC DECRA Fellowship under the supervision of Prof. Zaiping Guo at the University of Wollongong, Australia. Her research focuses on the advanced materials/electrochemistry characterization/interfacial electrochemistry for rechargeable batteries and efficient electrocatalysis.



Xinyu Zhao is currently an associate professor in Shandong University of Technology. He received his Ph.D. from the Shanghai Institute of Ceramics, Chinese Academy of Sciences in 2014. He continued his career as a postdoctoral research fellow at the Singapore University of Technology and Design and the University of Wollongong. His expertise lies in the design and controlled synthesis of functional inorganic nanomaterials and polymer-inorganic nanocomposites. His current research includes the synthesis and application of functional nanomaterials for energy devices.



Zaiping Guo is currently a distinguished professor at the University of Wollongong, Australia. She received her Ph.D. in Materials Engineering from the University of Wollongong in December 2003. After her Australian Postdoctoral (APD) fellowship in the Institute for Superconducting & Electronic Materials, she joined the Faculty of Engineering and Information Sciences, University of Wollongong as a Lecturer in 2008, and was promoted to professor in 2012, and then distinguished professor in 2019. Her current research interests are mainly focused on energy storage applications, such as lithium/sodium/potassium ion batteries, and hydrogen storage, as well as electrochemistry characterization and computer modeling.